INTERNATIONAL JOURNAL FOR NUMERICAL METHODS IN ENGINEERING
Int. J. Numer. Meth. Engng. **43**, 785–819 (1998)

ON THE COMPLETENESS OF MESHFREE PARTICLE METHODS

T. BELYTSCHKO *, Y. KRONGAUZ, J. DOLBOW AND C. GERLACH
Department of Mechanical Engineering, Northwestern University, Evanston, IL 60208-3111, U.S.A.

ABSTRACT

The completeness of Smooth Particle Hydrodynamics (SPH) and its modifications is investigated. Completeness, or the reproducing conditions, in Galerkin approximations play the same role as consistency in finite-difference approximations. Several techniques which restore various levels of completeness by satisfying reproducing conditions on the approximation or the derivatives of the approximation are examined. A Petrov–Galerkin formulation for a particle method is developed using approximations with corrected derivatives. It is compared to a normalized SPH formulation based on kernel approximations and a Galerkin method based on moving least-square approximations. It is shown that the major difference is that in the SPH discretization, the function which plays the role of the test function is not integrable. Numerical results show that approximations which do not satisfy the completeness and integrability conditions fail to converge for linear elastostatics, so convergence is not expected in non-linear continuum mechanics. © 1998 John Wiley & Sons, Ltd.

KEY WORDS: EFG; SPH; particle methods; meshfree; completeness; consistency

1. INTRODUCTION

The Smooth Particle Hydrodynamics (SPH) method pioneered by Gingold and Monaghan[1] has the potential to provide a robust, meshfree method for the analysis of continuum mechanics problems. However, in spite of its long history, the completeness of the approximations of the SPH method has not been examined extensively. In this paper, the smooth particle hydrodynamics method and its modifications are investigated from the viewpoint of completeness, which is closely related to consistency. Several procedures for correcting the lack of completeness of the original SPH are examined in this paper. Methods for the correction of this deficiency in SPH have previously been proposed by Liu *et al.*,[2] Johnson and Beissel,[3] Randles and Libersky[4] and Dilts.[5]

In Liu *et al.*,[2] a completeness correction was proposed for the SPH, which as shown in Belytschko *et al.*[6] leads to an approximation identical to the moving least-squares approximation. Johnson and Beissel[3] propose a method for modifying the derivatives of SPH for improved accuracy. Dilts[5] has enhanced SPH with a moving least-squares approximation. Other meshfree

* Correspondence to: T. Belytschko, Department of Mechanical Engineering, Northwestern University, 2145 Sheridan Road, Evanston, IL 60208-3111, U.S.A. E-mail: t-belytschko@nwu.edu

Contract/grant sponsor: Office of Naval Research
Contract/grant sponsor: US Army Office of Research
Contract/grant sponsor: DOE Computational Science Graduate Fellowship
Contract/grant sponsor: Army High Performance Computing Research Center; Contract/grant number: DAAH-04-95-2-003

CCC 0029–5981/98/050785–35$17.50

Received 15 November 1997
Revised 1 March 1998

methods with correction for improved convergence have recently been reported. Belytschko *et al.*[7] presented a convergent meshfree method based on a moving least-squares approximation. Krongauz and Belytschko[8] have developed a modification of the derivatives which meets the completeness requirements for second-order partial differential equations.

In this paper, the completeness of particle methods is examined. Completeness is satisfied if the approximation or its derivatives meets certain reproducing conditions. The reproducing conditions play the same role in the convergence of Galerkin approximations that consistency plays in finite-difference approximations. Several methods for meeting these reproducing conditions are described, one of which is presented for the first time in this paper. The methods of Johnson and Beissel[3] and Monaghan[9] are shown to lack the linear reproducing properties needed for convergence by a counterexample.

Two types of corrections are examined: those which correct the approximating functions, and those which correct the derivatives. The latter are computationally quicker. The discretization of the momentum equation for non-linear continuum mechanics by kernel and Galerkin methods is then described. The Galerkin discretization based on corrected derivatives requires different test and trial functions, since Krongauz and Belytschko[8] have shown that the test functions must be integrable. It is also shown that approximations which satisfy the reproducing conditions ensure conservation of linear and angular momentum for the discrete equations.

The consequences of using approximations which lack completeness are illustrated by numerical results. It is shown that discretizations which do not satisfy the requisite reproducing conditions do not converge for linear elasticity. On the other hand, the three methods which satisfy the requisite reproducing conditions exhibit convergence for linear elastic problems. Convergence in linear elastostatics is necessary if the discretization is to be convergent for non-linear solid mechanics problems.

The paper is organized as follows. In Section 2, we review the concepts of consistency, polynomial completeness, reproducing conditions, and integrability. In Section 3, the kernel approximation used in particle methods is reviewed. In Section 4 several methods for the completeness correction of the kernel approximation are reviewed; each of the correction methods is examined as to the degree of completeness met. In Section 5, the discretization of the non-linear continuum mechanics is summarized; the reproducing conditions which assure completeness in Galerkin methods are specified and the completeness of various schemes is investigated. In Section 6, the conclusions of Section 5 are verified by numerical studies and the accuracy and rates of convergence of alternative particle methods is examined.

2. CONSISTENCY, COMPLETENESS AND REPRODUCING CONDITIONS

Three terms are frequently used in the study of convergence:

1. Consistency of a discretization of a PDE, which is usually applied to finite-difference approximations.
2. Reproducing conditions, which is the ability of the approximation to reproduce specified functions which are usually polynomials.
3. Polynomial completeness, or completeness, see Reference 10.

Consistency is used mainly in finite-difference methods and is based on the truncation error obtained by a Taylor series expansion. The other two concepts are used in Galerkin methods for

convergence proofs and element tests such as the patch test in finite element methods. The reproducing conditions (or completeness) in Galerkin methods play the same role as consistency in finite-difference methods.

2.1. Consistency

In the finite-difference literature the consistency of an approximation is defined by its ability to exactly represent the differential equation in the limit as the number of grid points goes to infinity and the maximum distance between neighbouring grid points goes to zero. Strikwerda[11] defines consistency as follows.

Definition. A scheme $L_h u = f$ *that is consistent with the differential equation* $Lu = f$ *is accurate* (*consistent*) *of order* p *if for any sufficiently smooth function* v

$$Lv - L_h v = O(h^p) \tag{1}$$

where p is the order of consistency. For convergence, it is necessary that $p > 0$; generally, we require that $p \geqslant 1$. In the above definition, h is a parameter that reflects the refinement of the grid/mesh. If the mesh is regular, then h is the distance between grid points (nodes).

Consistency is an important ingredient of convergence. According to the famous Lax–Richtmyer equivalence theorem, *a consistent finite-difference scheme for a well-posed partial differential equation is convergent if and only if it is stable*, so consistency plus stability implies convergence.

2.2. Completeness and reproducing conditions

Ascertaining whether a meshfree method is consistent for an unstructured grid of nodes is quite difficult, as compared to checking whether a finite-difference scheme for a uniform grid is consistent. Therefore, we have chosen to examine the reproducing conditions, i.e. completeness, instead.

An approximation $u^h(x)$ is complete to order k if any polynomial up to order k can be represented exactly. Thus if $u^h(x)$ is given by

$$u^h(x) = \sum_I \Phi_I(x) u_I \tag{2}$$

where $\Phi_I(x)$ are the approximating functions and u_I are the nodal values, then if u_I are given by a polynomial of order k, the approximation $u^h(x)$ should reproduce the polynomial exactly if the approximation is complete to order k. These have come to be known as reproducing conditions in the literature on wavelets. In one dimension, the reproducing conditions can be written as follows. If the nodal values are given by a polynomial, i.e.

$$u_I = a_0 + a_1 x_I + a_2 x_I^2 + \cdots + a_k x_I^k \tag{3}$$

then the reproducing conditions (and completeness) of order k are met if

$$u^h(x) = \sum_I \Phi_I(x) u_I = a_0 + a_1 x + a_2 x^2 + \cdots + a_k x^k \tag{4}$$

Since the above must hold for arbitrary a_i, one can obtain the following conditions:

$$\sum_I \Phi_I(x) = 1 \tag{5a}$$

$$\sum_I \Phi_I(x) x_I = x \tag{5b}$$

$$\sum_I \Phi_I(x) x_I^2 = x^2 \tag{5c}$$

$$\cdots$$

$$\sum_I \Phi_I(x) x_I^k = x^k \tag{5d}$$

In two dimensions, the linear reproducing conditions can be written as

$$\sum_I \Phi_I(\mathbf{x}) = 1 \quad \sum_I \Phi_I(\mathbf{x}) x_I = x \quad \sum_I \Phi_I(\mathbf{x}) y_I = y \tag{6}$$

or in indicial notation

$$\sum_I \Phi_I(\mathbf{x}) x_{I\alpha} = x_\alpha \tag{7}$$

where $x_0 = x_{I0} = 1$, $x_1 = x$, $x_2 = y$, $x_{I1} = x_I$, $x_{I2} = y_I$.

Some corrections of particle methods are achieved by requiring that the derivatives of a polynomial field be correctly reproduced. We call these the derivative reproducing conditions. In two dimensions, the derivative reproducing conditions for a linear field are

$$\sum_I \Phi_{I,x}(\mathbf{x}) = 0, \quad \sum_I \Phi_{I,y}(\mathbf{x}) = 0 \tag{8a}$$

$$\sum_I \Phi_{I,x}(\mathbf{x}) x_I = 1, \quad \sum_I \Phi_{I,y}(\mathbf{x}) x_I = 0 \tag{8b}$$

$$\sum_I \Phi_{I,x}(\mathbf{x}) y_I = 0, \quad \sum_I \Phi_{I,y}(\mathbf{x}) y_I = 1 \tag{8c}$$

These can be obtained directly from equations (6) by taking their derivatives. In general, the linear derivative reproducing conditions for functions can be written as

$$\sum_I \Phi_{I,i} = 0 \tag{9a}$$

$$\sum_I \Phi_{I,i} x_{Ij} = \delta_{ij} \tag{9b}$$

Completeness replaces consistency in the convergence analysis of finite element (or more generally Galerkin) methods because of the way convergence is shown for Galerkin methods. Consider a differential equation $Lu = f$ with homogeneous boundary conditions on the first m derivatives where L is a self-adjoint differential operator of order $2m$. Then this differential equation (also referred to as the *strong form*) can be rewritten as a *weak form*

$$a(u, v) = (f, v) \quad \forall v \in H_0^m \tag{10}$$

where $a(u, v)$ is a bilinear differential operator in which m derivatives have been shifted from u to v by integration by parts and H_0^m is the space of functions possessing m square integrable

derivatives (in addition, it is required that the functions as well as their normal derivatives up to order $m-1$ vanish on the essential boundary). Problem statement (10) involves lower orders of derivatives than the strong form.

The problem (10) is discretized as follows. Find $u^h \in \mathscr{V}^h$ such that

$$a(u^h, v^h) = (f, v^h) \quad \forall v^h \in \mathscr{V}_0^h \tag{11}$$

where $\mathscr{V}_h$ and $\mathscr{V}_h^0$ are spaces that approximate the spaces H^m and H_0^m, respectively.

It is well known that for a self-adjoint problem, the solutions u^h of (10) are optimal in the natural (energy) norm, see Strang and Fix,[12] i.e.

$$a(u-u^h, u-u^h) = \min_{w^h \in \mathscr{V}^h} a(u-w^h, u-w^h) \tag{12}$$

The energy norm is equivalent to the norm of the Hilbert space H^m, i.e. there exist constants C_1 and C_2 such that for any $u \in H^m$

$$C_1 \|u\|_m \leqslant a(u,u)^{1/2} \leqslant C_2 \|u\|_m \tag{13}$$

Furthermore, the error is orthogonal to any function from the solution space, i.e.

$$a(u-u^h, v^h) = 0 \quad \forall v^h \in V_h \tag{14}$$

This condition, which does not hold for general differential equations, particularly when they are not self-adjoint (e.g. advection–diffusion), guarantees the stability of Galerkin methods. When (14) is satisfied and the discrete spaces are complete up to necessary order, convergence is assured.

Equation (12) allows one to establish bounds on the error in the energy norm by using interpolation energy norm estimates as an upper bound. The Nitsche trick (see Reference 12) makes it possible to obtain error bounds in the L_2 (displacement) norm. For a second-order differential equation the results are

$$a(e,e)^{1/2} = O(h^k) \tag{15a}$$

$$\|e\|_0 = O(h^{k+1}) \tag{15b}$$

$$e = u - u^h \tag{15c}$$

where k is the order of completeness of the approximation. The reproducing conditions are used to establish interpolation energy norm estimates which serve as upper bounds in the above. Thus it can be seen that in the analysis for convergence the role of completeness (i.e. reproducing conditions) in Galerkin methods parallels the role of consistency in finite-difference methods.

2.3. *Integrability of derivatives*

Another concept that is used frequently in this paper is integrability. Suppose in two dimensions we choose to approximate the derivatives of a function $u(\mathbf{x})$ by

$$u^h_{,x}(\mathbf{x}) = \sum_I f_I(\mathbf{x}) u_I \tag{16}$$

$$u^h_{,y}(\mathbf{x}) = \sum_I g_I(\mathbf{x}) u_I \tag{17}$$

Then we will say that f_I and g_I are integrable if

$$f_{I,y} = g_{I,x} \tag{18}$$

Integrability implies the existence of a function $E_I(\mathbf{x})$ such that $E_{I,x}(\mathbf{x}) = f_I(\mathbf{x})$ and $E_{I,y}(\mathbf{x}) = g_I(\mathbf{x})$. Some derivative approximations that are to be presented subsequently will not meet this condition.

3. APPROXIMATIONS IN MESHFREE METHODS

Most meshfree methods are based on the use of an approximating function which is non-zero only in a small neighbourhood of a point I, i.e. a function with compact support. The compactness of the support is essential for the sparsity of the discrete equations. In SPH, this function is called the kernel function or smoothing function; it will be denoted by $W(\mathbf{x})$ where $\mathbf{x} = (x, y)$ in two dimensions. In methods based on Moving Least-Square (MLS) approximations the function is called a weight function and is denoted by $w(\mathbf{x})$.

SPH approximations are based on a continuous kernel approximation

$$u^h(\mathbf{x}, t) = \int_\Omega W(\mathbf{x} - \mathbf{y}, s(\mathbf{y}, t)) u(\mathbf{y}, t)\, \mathrm{d}\Omega_y \tag{19}$$

where Ω is the domain of the problem (the integral can be restricted to the compact support of the kernel) and $s(\mathbf{y}, t)$ is the smoothing length which can vary both in space and time. The kernel W in (19) is usually required to satisfy

$$\int_\Omega W(\mathbf{y}, s(\mathbf{y}, t))\, \mathrm{d}\Omega_y = 1 \tag{20}$$

A discrete approximation (by a simple integration based on nodal values) of the integral (19), yields the SPH approximation $u^h(\mathbf{x}, t)$

$$u^h(\mathbf{x}, t) \cong \sum_I W(\mathbf{x} - \mathbf{x}_I, s(\mathbf{x}_I, t)) u_I(t)\, \Delta V_I \tag{21}$$

where ΔV_I is the area or volume associated with node I. The smoothing length can also be a function $s(\mathbf{x}, t)$ so that

$$u^h(\mathbf{x}, t) = \int_\Omega W(\mathbf{x} - \mathbf{y}, s(\mathbf{x}, t)) u(\mathbf{y}, t)\, \mathrm{d}\Omega_y \tag{22}$$

which leads to the discrete SPH approximation of the form

$$u^h(\mathbf{x}, t) \cong \sum_I W(\mathbf{x} - \mathbf{x}_I, s(\mathbf{x}, t)) u_I(t)\, \Delta V_I \tag{23}$$

The difference between (21) and (23) is that in (21) the domain of influence of a node is always circular and thus the weight is only a function of $d = \|x - x_I\|$, the distance to the node; furthermore, in taking the gradient of $u^h(x, t)$ extra terms appear in (21) but not in (23). On the other hand, in (23) the weight depends not only on the distance to the node but also on the position of the evaluation point ($\mathbf{x}$) with respect to the node. In all the numerical examples we have used circular domains of influence (i.e. equation (21) rather than equation (23)). In the subsequent equations, we will not explicitly state the functional dependence of the approximation on s or time t.

SPH approximations are typically constructed only at the nodes,

$$u^h(\mathbf{x}_J) = \sum_I W_{JI} u_I \, \Delta V_I \tag{24}$$

where the definition

$$W_{JI} \equiv W(\mathbf{x}_J - \mathbf{x}_I) \tag{25}$$

will be used for brevity throughout this paper.

A typical kernel function is the B-spline

$$W(q,s) = \frac{2}{3s} \begin{cases} 1 - \frac{3}{2}q^2 + \frac{3}{4}q^3 & \text{for } q \leqslant 1 \\ \frac{1}{4}(2-q)^3 & \text{for } 1 \leqslant q \leqslant 2 \\ 0 & \text{for } q \geqslant 2 \end{cases} \tag{26}$$

in one dimension where $q = \|x - x_I\|/s$; the radius of the support of this kernel is $2s$.

The development of the discrete form of the gradient of a function in SPH begins with the continuous form. Similar to the kernel approximation of a function, equation (19), the kernel approximation of the gradient of a function is given by

$$\nabla u^h(\mathbf{x}) = \int_\Omega W(\mathbf{x} - \mathbf{y}) \nabla u(\mathbf{y}) \, \mathrm{d}\Omega_y \tag{27}$$

Integrating this expression by parts gives

$$\nabla u^h(\mathbf{x}) = \int_\Gamma W(\mathbf{x} - \mathbf{y}) u(\mathbf{y}) \mathbf{n} \, \mathrm{d}\Gamma - \int \nabla W(\mathbf{x} - \mathbf{y}) u(\mathbf{y}) \, \mathrm{d}\Omega_y \tag{28}$$

The surface term is usually neglected in SPH with the argument that either the kernel W or the function u vanishes on the boundary. (These conditions are often not met, which perhaps leads to problems in accuracy. Such inconsistencies do not occur in Galerkin approximations.) The discrete representation for the gradient of a function is then given by

$$\nabla u^h(\mathbf{x}) \cong - \sum_I \nabla W(\mathbf{x} - \mathbf{x}_I) u_I \, \Delta V_I \tag{29}$$

or at a given node

$$\nabla u^h(\mathbf{x}_J) = - \sum_I \nabla W_{JI} u_I \, \Delta V_I \tag{30}$$

where in the last expression we have used the notation $\nabla W_{JI} = \nabla W(\mathbf{x}_J - \mathbf{x})|_{x_I}$. For a symmetric kernel W with a spatially uniform support s, the following identity holds:

$$\nabla u(\mathbf{x}_J) = - \sum_I \nabla W_{JI} u_I \Delta V_I = \sum_I \nabla W_{IJ} u_I \Delta V_I \tag{31}$$

since $\nabla W_{JI} = -\nabla W_{IJ}$.

The discrete forms of the kernel approximation to a function (21) and its gradient (29) are similar to shape function approximation in the finite element method. For example, (21) can be rewritten as

$$u^h(\mathbf{x}) = \sum_I \Phi_I(\mathbf{x}) u_I \tag{32}$$

where the approximation functions $\Phi_I(\mathbf{x})$ given by

$$\Phi_I(\mathbf{x}) = W(\mathbf{x} - \mathbf{x}_I)\Delta V_I \tag{33}$$

play the same role as the shape functions in finite elements. However, the kernel approximations are not interpolants, i.e.

$$W(\mathbf{x}_J - \mathbf{x}_I)\Delta V_I \neq \delta_{IJ} \tag{34}$$

so the nodal variables u_I do not correspond to $u^h(\mathbf{x}_I)$, i.e. $u_I \neq u^h(\mathbf{x}_I)$.

Taking the gradient of (32) gives

$$\nabla u^h(\mathbf{x}) = \sum_I \nabla \Phi_I(\mathbf{x}) u_I \tag{35}$$

When the gradient terms are evaluated at a node

$$\nabla \Phi_I(\mathbf{x}_J) = \nabla \Phi(\mathbf{x} - \mathbf{x}_I)|_{x_J} \tag{36}$$

which is equivalent to (29) if W_{IJ} is symmetric and has a spatially uniform smoothing length.

Even when the kernel satisfies (20), its discrete counterpart (24) does not necessarily reproduce constant functions for an unstructured set of particles, i.e

$$\sum_I W(\mathbf{x} - \mathbf{x}_I)\Delta V_I \neq 1 \tag{37}$$

does not hold. Thus the standard SPH approximation lacks zeroth order completeness and convergence of Galerkin methods for even self-adjoint PDEs of first order cannot be proven by standard methods.

4. CORRECTION OF KERNEL APPROXIMATIONS

Completeness can be restored in kernel approximations through a correction transformation. It is easier to develop these transformations by enforcing the reproducing conditions than to enforce consistency by correcting the truncation error, so this approach is taken here.

Completeness corrections of two types have evolved:

1. completeness corrections of the approximating functions;
2. completeness corrections of the derivatives of approximating functions.

For correction of the approximating functions, a correction which provides for constant reproducing conditions is given by Shepard.[13] A more complete correction which provides for linear reproducing conditions corresponds to the moving least-squares approximation, Belytschko *et al.*[14]

For derivative corrections, several approaches are examined:

1. the symmetrization given in Monaghan;[15]
2. the Johnson and Beissel[3] correction;
3. the Randles and Libersky[4] renormalization;
4. the corrections given in Krongauz and Belytschko;[8]
5. a new correction based on Krongauz and Belytschko.[8]

We will first describe corrections of the approximation functions, followed by a description and examination of corrections for derivatives of approximations.

4.1. Correction of the approximation function

The first approach to insuring completeness in kernel approximations is to correct the approximation function so that it satisfies the required reproducing conditions. After the correction is made on the approximation, the derivatives of the approximation will satisfy the corresponding derivative reproducing conditions.

4.2. Constant completeness—Shepard functions

An approximation widely used in fitting data proposed by Shepard[13] is

$$u^h(\mathbf{x}) = \sum_I w_I^{\mathrm{S}}(\mathbf{x}) u_I \tag{38}$$

where

$$w_I^{\mathrm{S}}(\mathbf{x}) = \frac{w_I(\mathbf{x})}{\sum_J w_J(\mathbf{x})} \tag{39}$$

where $w_J(d) \geqslant 0$ in a subdomain $\Omega_J \subset \Omega$, i.e. $w_J(d)$ has compact support. The same functions used for kernels can be used for weight functions, e.g. the B-spline defined in (26).

It can be seen that Shepard functions reproduce constant functions: when $u_I = c \ \forall I$, then

$$u^h(x) = \sum_I w_I^{\mathrm{S}}(x) u_I \tag{40}$$

$$= \sum_I w_I^{\mathrm{S}}(x) \cdot c \tag{41}$$

$$= \frac{\sum_I w_I(x)}{\sum_J w_J(x)} c = c \tag{42}$$

They will also correctly reproduce the gradients of a constant function, i.e. $u^h_{,i}(x) = 0$, so (8a) is met and the derivative for a constant function is reproduced exactly.

If $w(\mathbf{x})$ are C^n, then the Shepard approximant $w^{\mathrm{S}}(\mathbf{x})$ is also C^n. Thus, the weight functions (26) lead to Shepard approximants which are C^2. An advantage of the Shepard approximants is that they can be computed at relatively low cost.

4.3. Linear completeness—moving least squares

Linear completeness can be obtained either by using a moving least-squares approximation, as succinctly shown in Reference 16 or by adding a correction function to the kernel approximation.[2] The MLS approach is not a correction but directly computes approximations with a specified level of completeness; however, an approximation equivalent to MLS can be constructed by correcting a kernel function; the two approaches are equivalent (see Reference 6). In this paper, to highlight the similarity to subsequent developments on completeness corrections for the derivatives, we use the second approach and illustrate it for first-order completeness.

The ability to reproduce linear functions is imparted to the approximation by modifying it by a linear function $\beta_\alpha(\mathbf{x})\mathbf{x}_\alpha$, i.e. we let

$$u^h(\mathbf{x}) = \sum_I \Phi_I(\mathbf{x}) u_I \tag{43}$$

where

$$\Phi_I(\mathbf{x}) = \beta_\alpha(\mathbf{x}) x_{I\alpha} w_I(\mathbf{x}) \tag{44}$$

which can be seen to be a modification of (21) and (38). Here the Greek indices have a range 0 to the number of spatial dimensions (n_{SD}) and $x_0 = 1$.

The reproducing conditions (6) then yield the following equations for the coefficients $\beta_\alpha(\mathbf{x})$:

$$\sum_I (x_{I\alpha} w_I(\mathbf{x}) x_{I\gamma}) \beta_\alpha(\mathbf{x}) = \delta_{\alpha\gamma} \tag{45}$$

when *the co-ordinate system is shifted to the point of evaluation*, i.e. $\mathbf{x} = 0$. For example, in two dimensions the equations for $\beta_\alpha(\mathbf{x})$ are given by

$$\boldsymbol{\beta}(0) = \left(\sum_I w_I(\mathbf{x}) \begin{bmatrix} 1 & x_I - x & y_I - y \\ x_I - x & (x_I - x)^2 & (x_I - x)(y_I - y) \\ y_I - y & (x_I - x)(y_I - y) & (y_I - y)^2 \end{bmatrix} \right)^{-1} \begin{bmatrix} 1 \\ 0 \\ 0 \end{bmatrix} \tag{46}$$

The shifting of the origin improves the conditioning of the above matrix and thus reduces the roundoff error. The resulting approximation reproduces linear functions by construction.

4.4. Correction of the derivatives of approximations

It is also possible to correct the derivatives of the approximation directly, without necessarily restoring the completeness of the approximating functions. This is achieved by modifying the approximation to the derivatives to satisfy the derivative reproducing conditions, equation (8). These derivative completeness corrections are usually implemented through linear transformations of the original derivatives.

4.4.1. Zeroth-order derivative completeness condition

The simplest derivative completeness corrections of particle approximations are for zeroth-order completeness. To obtain zeroth-order completeness, the approximation must be able to reproduce the correct derivative for a constant function, i.e. if $u_I = 1 \ \forall I$ then $u^h_{,i}(x) = 0$.

The simplest correction for the derivatives is the symmetrization proposed by Monaghan[15] (it is actually a skew-symmetric form). Although this form has been used specifically in the momentum equation for stability reasons,[17] it can be used to calculate the gradient of any function. For example, this modification applied to the standard SPH formula for the gradient of a function (29) gives

$$\nabla u^h(\mathbf{x}_J) = -\sum_I \nabla W_{JI}(u_I - u_J) \Delta V_I \tag{47}$$

It is easy to see from (47) that when $u(\mathbf{x})$ is constant then $u_I = u_J \ \forall I,J$ and the derivatives must vanish.

When compared to the zeroth-order approximating function correction of Shepard of Section 4.2, equation (47) appears to be equally effective from the viewpoint of computational effort; this is discussed further in Section 6. However, the Shepard correction is valid at any point in the domain, whereas the symmetrization correction can only be imposed at the nodes. More importantly, in the Shepard correction, the derivatives are integrable since they emanate from a well-defined

function (38). The symmetrization correction (47) modifies the derivatives of an approximation, and thus they are usually not integrable. Krongauz and Belytschko[8] reported that *non-integrable test function derivatives lead to a failure of convergence* in Galerkin methods.

4.4.2. Johnson–Beissel correction

Johnson and Beissel[3] have proposed a correction of the derivatives of SPH approximations for linear functions. They consider the case of axisymmetry; here we present the equations for the Cartesian case for the sake of simplicity. The correction is directly applied to the expressions for the rate of deformation, so we follow the same description. The original SPH expressions with the symmetrization correction for the normal velocity strains, D_x, D_y are given by

$$D_x(\mathbf{x}_J) = v_{x,x} = -\sum_I \frac{\partial W_{JI}}{\partial x}\Delta V_I(v_{xI} - v_{xJ}) \tag{48a}$$

$$D_y(\mathbf{x}_J) = v_{y,y} = -\sum_I \frac{\partial W_{JI}}{\partial y}\Delta V_I(v_{yI} - v_{yJ}) \tag{48b}$$

It can be seen from (48) that the normal velocity strains vanish when all velocities are the same (i.e. constant reproducing conditions on derivatives) However, for the case of a linear distribution of velocities, the strain rates will not necessarily be constant, (i.e. the linear reproducing conditions on the derivatives are not satisfied).

Johnson and Beissel[3] have proposed the following modification to the computation of strain rates. Let the normal strain rates be computed by

$$D_x(\mathbf{x}_J) = -\sum_I \beta_x \frac{\partial W_{JI}}{\partial x}\Delta V_I(v_{xI} - v_{xJ}) \tag{49a}$$

$$D_y(\mathbf{x}_J) = -\sum_I \beta_y \frac{\partial W_{JI}}{\partial y}\Delta V_I(v_{yI} - v_{yJ}) \tag{49b}$$

The difference between (49) and (48) is in the correction factors β_x and β_y. For each node the factors are adjusted so that for velocity fields which yield constant values of D_x and D_y, the velocity strains are reproduced exactly by (49). No modifications are made on the shear rate.

For the case of a constant D_x, we have

$$(x_I - x_J)D_x = v_{xI} - v_{xJ} \tag{50}$$

Substituting (50) into (49a) we obtain

$$D_x = -\sum_I \beta_x \frac{\partial W_{JI}}{\partial x}\Delta V_I D_x(x_I - x_J) \tag{51}$$

The velocity strain, D_x, cancels on both sides so β_x is

$$\beta_x = -\frac{1}{\sum_I \frac{\partial W_{JI}}{\partial x}\Delta V_I(x_I - x_J)} \tag{52a}$$

Similarly,

$$\beta_y = -\frac{1}{\sum_I \frac{\partial W_{JI}}{\partial y}\Delta V_I(y_I - y_J)} \tag{52b}$$

The modified derivatives (49) are still not able to reproduce the derivatives of arbitrary linear velocity fields. Consider a velocity field for the x given by

$$v_x = \alpha_1(x + y) \tag{53a}$$

$$v_y = \alpha_2(x + y) \tag{53b}$$

It is clear that the velocity strains are constant and $D_x = \alpha_1$ and $D_y = \alpha_2$. However, if the expressions for v_x, (53a), and β_x, (52a), are substituted into (49a), we obtain

$$\begin{aligned} D_x &= \alpha_x \frac{\sum_I \frac{\partial W_{JI}}{\partial x} \Delta V_I((x_I - x_J) + (y_I - y_J))}{\sum_I \frac{\partial W_{JI}}{\partial x} \Delta V_I(x_I - x_J)} \\ &= \alpha_x \left(1 + \frac{\sum_I \frac{\partial W_{JI}}{\partial x} \Delta V_I(y_I - y_J)}{\sum_I \frac{\partial W_{JI}}{\partial x} \Delta V_I(x_I - x_J)} \right) \end{aligned} \tag{54}$$

where the second term in the parenthesis is, in general, not equal to zero. Thus, this correction does not ensure that the approximation is able to reproduce the correct derivatives of arbitrary linear functions. However, numerical tests reported in Reference 3 show improved results using this correction as compared to (48).

4.4.3. Krongauz–Belytschko correction, Method 1

Krongauz and Belytschko[8] developed a completeness correction in which the derivatives are reproduced exactly for any constant or linear fields. They referred to the corrected derivatives as pseudo-derivatives because the corrected derivatives of shape functions, in general, are not integrable. We will refer to them as corrected derivatives henceforth; Randles and Libersky[4] use the term normalized derivatives.

In this correction the corrected derivatives are denoted by $G_{iI}(\mathbf{x})$

$$u_{,i}^h(\mathbf{x}) = \sum_I G_{iI} u_I \tag{55}$$

where the G_{iI} are linear combinations of the derivatives of the Shepard functions, i.e.

$$G_{iI}(\mathbf{x}) = \alpha_{ij}(\mathbf{x}) w_{I,j}^{\mathrm{S}}(\mathbf{x}) \quad \text{or} \quad \mathbf{G}_I = \boldsymbol{\alpha} \cdot \boldsymbol{\nabla} w_I^{\mathrm{S}}(\mathbf{x}) \tag{56}$$

In two dimensions the above gives

$$G_{Ix} = \alpha_{11} w_{I,x}^{\mathrm{S}}(\mathbf{x}) + \alpha_{12} w_{I,y}^{\mathrm{S}}(\mathbf{x}) \tag{57a}$$

$$G_{Iy} = \alpha_{21} w_{I,x}^{\mathrm{S}}(\mathbf{x}) + \alpha_{22} w_{I,y}^{\mathrm{S}}(\mathbf{x}) \tag{57b}$$

Since the Shepard functions satisfy zeroth-order completeness, the modified gradients G_{iI} automatically satisfy zeroth-order completeness.

The correction coefficients α_{ij} are obtained by imposing the reproducing conditions on the derivatives of linear functions, equation (8). Thus, if we let $u_i^h(\mathbf{x}) = x_i$, then the reproducing condition

for the derivatives, equation (8), requires

$$u^h_{,j}(\mathbf{x}) = \sum G_{jI}(\mathbf{x}) u_I = \sum G_{jI}(\mathbf{x}) x_{Ii} \tag{58}$$

$$= \sum \alpha_{jk} w^{\mathrm{S}}_{I,k}(\mathbf{x}) x_{Ii} = \delta_{ij} \tag{59}$$

where equation (56) has been substituted for G_{jI}. The above yields n_{SD} sets of n_{SD} equations in the unknowns α_{ij}, where n_{SD} refers to the number of spatial dimensions. By solving these equations, the expressions (56) for the gradient G_{iI} can be evaluated and the approximation for the derivatives is then obtained by (55).

In two dimensions, for example, the linear algebraic equations for the derivative correction factors are

$$\mathbf{A}\boldsymbol{\alpha} = \mathbf{I} \tag{60}$$

where $\mathbf{I}$ is the identity matrix and

$$\mathbf{A} = \sum_I \begin{bmatrix} w^{\mathrm{S}}_{I,x} x_I & w^{\mathrm{S}}_{I,y} x_I \\ w^{\mathrm{S}}_{I,x} y_I & w^{\mathrm{S}}_{I,y} y_I \end{bmatrix} \tag{61}$$

This correction results in a gradient operator which reproduces the derivatives of constant and linear functions exactly. Therefore, the approximation for the gradient satisfies first-order completeness. In computations, the origin should be shifted to $\mathbf{x}$ to improve the conditioning of the $\mathbf{A}$ matrix and reduce round-off error. The velocity gradient is then computed by

$$v_{i,j}(\mathbf{x}) = \alpha_{jk} w^{\mathrm{S}}_{I,k} \dot{u}_{Ii} \tag{62}$$

However, the resulting derivatives are not integrable. Therefore, they are not suitable as test functions in Galerkin methods. However, in a Petrov–Galerkin-type formulation, these derivatives can be used as trial functions with Shepard functions as test functions, which has been shown to be effective in a Petrov–Galerkin-type formulation of elasticity, see Reference 8 for details.

4.4.4. Correction of derivatives. Method 2

The corrected derivatives can also be obtained by introducing a correction which in two dimensions takes the form

$$\Phi_I = (\alpha_{11}(\mathbf{x}) + \alpha_{12}(\mathbf{x}) x_I + \alpha_{13}(\mathbf{x}) y_I) w^{\mathrm{S}}_I(\mathbf{x}) \tag{63a}$$

$$G_{Ix} = (\alpha_{21}(\mathbf{x}) + \alpha_{22}(\mathbf{x}) x_I + \alpha_{23}(\mathbf{x}) y_I) w^{\mathrm{S}}_I(\mathbf{x}) \tag{63b}$$

$$G_{Iy} = (\alpha_{31}(\mathbf{x}) + \alpha_{32}(\mathbf{x}) x_I + \alpha_{33}(\mathbf{x}) y_I) w^{\mathrm{S}}_I(\mathbf{x}) \tag{63c}$$

If the co-ordinate system is shifted to the point of evaluation $\mathbf{x}$ then the coefficients $\boldsymbol{\alpha}$ are then obtained according to (60) with $\mathbf{A}$ given by

$$\mathbf{A} = \sum_I w^{\mathrm{S}}_I(\mathbf{x}) \begin{bmatrix} 1 & x_I - x & y_I - y \\ x_I - x & (x_I - x)^2 & (x_I - x)(y_I - y) \\ y_I - y & (x_I - x)(y_I - y) & (y_I - y)^2 \end{bmatrix} \tag{64}$$

In contrast to the method of Section 4.4.3, in two dimensions a 3×3 matrix needs to be inverted. An advantage of this method is the fact that linearly complete shape functions are obtained in

addition to corrected derivatives. It was shown in Krongauz and Belytschko[18] that this is equivalent to the Nayroles *et al.*[19] interpretation of the MLS approximation.

4.4.5. Correction of derivatives. Method 3

The third approach to obtaining linearly consistent (complete) shape function derivatives is as follows. Consider the two-dimensional case. Let us seek shape functions and shape function derivatives in the following form:

$$\bar{\Phi}_I(\mathbf{x}) = \alpha_{11}(\mathbf{x}) w^{\mathrm{S}}_{I,x}(\mathbf{x}) + \alpha_{12}(\mathbf{x}) w^{\mathrm{S}}_{I,y}(\mathbf{x}) + \alpha_{13}(\mathbf{x}) w^{\mathrm{S}}_{I}(\mathbf{x}) \tag{65a}$$

$$G_{Ix}(\mathbf{x}) = \alpha_{21}(\mathbf{x}) w^{\mathrm{S}}_{I,x}(\mathbf{x}) + \alpha_{22}(\mathbf{x}) w^{\mathrm{S}}_{I,y}(\mathbf{x}) + \alpha_{23}(\mathbf{x}) w^{\mathrm{S}}_{I}(\mathbf{x}) \tag{65b}$$

$$G_{Iy}(\mathbf{x}) = \alpha_{31}(\mathbf{x}) w^{\mathrm{S}}_{I,x}(\mathbf{x}) + \alpha_{23}(\mathbf{x}) w^{\mathrm{S}}_{I,y}(\mathbf{x}) + \alpha_{33}(\mathbf{x}) w^{\mathrm{S}}_{I}(\mathbf{x}) \tag{65c}$$

$\boldsymbol{\alpha}(\mathbf{x})$ are now obtained by requiring the approximation $\bar{\Phi}_I$ to reproduce linear functions and the derivatives G_{Ix} and G_{Iy} of the approximation to reproduce the derivatives of linear functions. To achieve this, (65) are substituted into (6) and (8). If the co-ordinate system is shifted to the point of evaluation $\mathbf{x}$ then the coefficients $\boldsymbol{\alpha}$ are then obtained according to (60) with $\mathbf{A}$ given by

$$\mathbf{A} = \sum_I \begin{pmatrix} w^{\mathrm{S}}_{I,x}(\mathbf{x}) & w^{\mathrm{S}}_{I,y}(\mathbf{x}) & w^{\mathrm{S}}_{I}(\mathbf{x}) \\ w^{\mathrm{S}}_{I,x}(\mathbf{x}) x_I & w^{\mathrm{S}}_{I,y}(\mathbf{x}) x_I & w^{\mathrm{S}}_{I}(\mathbf{x}) x_I \\ w^{\mathrm{S}}_{I,x}(\mathbf{x}) y_I & w^{\mathrm{S}}_{I,y}(\mathbf{x}) y_I & w^{\mathrm{S}}_{I}(\mathbf{x}) y_I \end{pmatrix} \tag{66}$$

Compared to the form of the corrected derivatives given in Section 4.4.3, the shape functions (65) are obtained at a slightly higher computational cost than (56) (due to having to invert a 3×3 rather than a 2×2 matrix in two dimensions). However, the shape functions themselves are able to reproduce linear functions rather than just constant functions in the case of (56).

4.4.6. Randles–Libersky correction

In Reference 4, a generalization of the ideas of Johnson and Beissel[3] is proposed which they attribute to Everhart. The approach is illustrated for the case of the divergence of a second-order tensor $\boldsymbol{\sigma}$. The usual form would be

$$(\boldsymbol{\nabla} \cdot \boldsymbol{\sigma})_J = -\sum_I (\boldsymbol{\sigma}_I - \boldsymbol{\sigma}_J) \cdot \boldsymbol{\nabla} W_{JI} \Delta V_I \tag{67}$$

This is modified as follows. Let

$$(\boldsymbol{\nabla} \cdot \boldsymbol{\sigma})_J = -\left(\sum_I (\boldsymbol{\sigma}_I - \boldsymbol{\sigma}_J) \otimes \boldsymbol{\nabla} W_{JI} \Delta V_I \right) : \mathbf{B} \tag{68}$$

where $\otimes$ denotes a tensor product. The components of $\mathbf{B}$ are found by requiring that (68) correctly compute the gradients of an arbitrary linear tensor field. This results in

$$\mathbf{B} = \left(-\sum_I (\mathbf{x}_I - \mathbf{x}_J) \otimes \boldsymbol{\nabla} W_{JI} \Delta V_I \right)^{-1} \tag{69}$$

If equation (31) is used, and $W_{JI}(\mathbf{x})\Delta V_I$ is replaced by the Shepard functions $w_I^{\mathrm{S}}(\mathbf{x}_J)$ this expression becomes

$$\mathbf{B} = \left(\sum_I \mathbf{x}_I \otimes \nabla w_I^{\mathrm{S}}(\mathbf{x}_J) \right)^{-1} \tag{70}$$

which in two dimensions is identical to the $\boldsymbol{\alpha}$ obtained from (60) at $\mathbf{x} = \mathbf{x}_J$. The symmetrization term $-\mathbf{x}_J$ in (69) does not appear in the above equation due to the constant completeness of the Shepard functions. Thus, the only difference between the two correction techniques is that one uses Shepard functions and the other symmetrization to satisfy the constant completeness requirement.

As mentioned in Section 4.4.1 these approximations to the derivatives are not integrable. This leads to an inability to satisfy the patch test when these approximations are used for both test and trial functions.[8]

4.4.7. Interpolation estimate

We present an interpolation estimate of the accuracy of the corrected derivatives in two dimensions. We will show that under reasonable assumptions, for derivative approximations which satisfy linear reproducing conditions, the errors in derivative interpolations are of order $O(h)$.

Let $u(\mathbf{x})$ be a function for which the following expansion around $\mathbf{x}$ is valid:

$$\begin{aligned} u(\mathbf{x}_I) = u(\mathbf{x}) + u_{,x}(\mathbf{x})(x_I - x) + u_{,y}(\mathbf{x})(y_I - y) + \tfrac{1}{2}u_{,xx}(\mathbf{x})(x_I - x)^2 \\ + u_{,xy}(\mathbf{x})(x_I - x)(y_I - y) + \tfrac{1}{2}u_{,yy}(\mathbf{x})(y_I - y)^2 + O(h^3) \end{aligned} \tag{71}$$

Ignoring higher-order terms we can write $u_{,x}^h(\mathbf{x}) - u_{,x}$ as

$$u_{,x}^h(\mathbf{x}) - u_{,x} = \sum_I G_{xI}(\mathbf{x})u_I - u_{,x} = \sum_I G_{xI}(\mathbf{x})u(\mathbf{x}_I) - u_{,x} \tag{72}$$

Substituting (71) into the above gives

$$\begin{aligned} u_{,x}^h(\mathbf{x}) - u_{,x} = u(\mathbf{x}) \sum_I G_{xI}(\mathbf{x}) + u_{,x}(\mathbf{x}) \left(\sum_I G_{xI}(\mathbf{x})(x_I - x) - 1 \right) \\ + u_{,y}(\mathbf{x}) \sum_I G_{xI}(\mathbf{x})(y_I - y) + \frac{1}{2}u_{,xx}(\mathbf{x}) \sum_I G_{xI}(\mathbf{x})(x_I - x)^2 \\ + u_{,xy}(\mathbf{x}) \sum_I G_{xI}(\mathbf{x})(x_I - x)(y_I - y) + \frac{1}{2}u_{,yy}(\mathbf{x}) \sum_I G_{xI}(\mathbf{x})(y_I - y)^2 \end{aligned} \tag{73}$$

The constant and linear derivative completeness of G_{xI} and G_{yI} yield, see equations (8):

$$\sum_I G_{xI} = 0 \tag{74a}$$

$$\sum_I G_{xI}(x_I - x) = 1 \tag{74b}$$

$$\sum_I G_{xI}(y_I - y) = 0 \tag{74c}$$

which simplifies (73) to

$$u^h_{,x}(\mathbf{x}) - u_{,x} = \frac{1}{2}u_{,xx}(\mathbf{x})\sum_I G_{xI}(\mathbf{x})(x_I - x)^2 + u_{,xy}(\mathbf{x})\sum_I G_{xI}(\mathbf{x})(x_I - x)(y_I - y) + \frac{1}{2}u_{,yy}(\mathbf{x})\sum_I G_{xI}(\mathbf{x})(y_I - y)^2 \tag{75}$$

From the above equation we obtain

$$|u^h_{,x}(\mathbf{x}) - u_{,x}| \leqslant \frac{1}{2}|u_{,xx}(\mathbf{x})|\left|\sum_I G_{xI}(\mathbf{x})(x_I - x)^2\right| + |u_{,xy}(\mathbf{x})|\left|\sum_I G_{xI}(\mathbf{x})(x_I - x)(y_I - y)\right| + \frac{1}{2}|u_{,yy}(\mathbf{x})|\left|\sum_I G_{xI}(\mathbf{x})(y_I - y)^2\right| \tag{76}$$

Since all of the shape functions have compact support, there exists a constant d_M such that for any $\mathbf{x} = (x, y)$

$$|x_I - x| \leqslant d_M, \quad |y_I - y| \leqslant d_M \tag{77}$$

Then

$$|u^h_{,x}(\mathbf{x}) - u_{,x}| \leqslant (\tfrac{1}{2}|u_{,xx}(\mathbf{x})| + |u_{,xy}(\mathbf{x})| + \tfrac{1}{2}|u_{,yy}(\mathbf{x})|)d_M^2 \sum_I |G_{xI}| \tag{78}$$

If we assume that G_{xI} satisfies

$$|G_{xI}| \leqslant \frac{C_1}{h} \tag{79}$$

then if the supports of shape functions are chosen so that the size of the support is proportional to the local refinement parameter h, i.e. $d_M \leqslant d_m h$, then

$$|u^h_{,x}(\mathbf{x}) - u_{,x}| \leqslant C(\tfrac{1}{2}|u_{,xx}(\mathbf{x})| + |u_{,xy}(\mathbf{x})| + \tfrac{1}{2}|u_{,yy}(\mathbf{x})|)h \tag{80}$$

So the approximation error in the derivative is of order h for a corrected derivative approximation. Similar observations hold for the y derivative.

5. CONTINUUM MECHANICS DISCRETIZATIONS

In a domain Ω bounded by Γ the governing equations in a Lagrangian description are

$$\text{Momentum equation:} \quad \rho\dot{\mathbf{v}} = \boldsymbol{\nabla}\cdot\boldsymbol{\sigma} + \mathbf{b} \quad \text{in } \Omega \tag{81}$$

$$\text{Constitutive equation:} \quad \overset{\nabla}{\boldsymbol{\sigma}} = \mathbf{C}:\mathbf{D} \quad \text{in } \Omega \tag{82}$$

$$\text{Velocity strain:} \quad \mathbf{D} = \boldsymbol{\nabla}^{\mathrm{S}}\mathbf{v} \tag{83}$$

where the first equation is expressed in terms of the velocity $\mathbf{v}$ and the Cauchy stress $\boldsymbol{\sigma}$. The density is denoted by ρ, $\mathbf{b}$ is the body force, $\boldsymbol{\nabla}^{\mathrm{S}}$ is the symmetric part of the gradient. The constitutive equation is expressed in terms of an objective stress rate and the rate of deformation

tensor **D**. The following boundary conditions are imposed on the displacement Γ_u and traction Γ_τ boundaries:

$$\boldsymbol{\sigma}\cdot\mathbf{n}=\mathbf{t} \quad \text{on } \Gamma_\tau \tag{84a}$$

$$\mathbf{u}=\bar{\mathbf{u}} \quad \text{on } \Gamma_u \tag{84b}$$

where $\Gamma=\Gamma_u\cup\Gamma_\tau$, and $\Gamma_u\cap\Gamma_\tau=0$.

We next consider the discretization of the momentum equation and the resulting completeness requirements. Two methods of discretization are commonly used in particle methods:

1. Collocation, in which the momentum equation is enforced at a discrete set of points; these points usually coincide with the same nodes that are used for the construction of the approximation; this is almost identical to a kernel approximation.
2. Galerkin methods, in which the discrete equations are obtained from a weak form of the momentum equation.

In SPH, collocation methods are usually used. Recent work with EFG and other methods based on moving least-squares approximations has focused on Galerkin methods. In this section, we will show that the discrete equations in SPH are similar to those of a Galerkin method with nodal quadrature. When completeness corrections are made to the derivatives of the approximations directly, a Petrov–Galerkin formulation is needed. If the test functions are not integrable the discretization does not converge, which will be illustrated in the numerical studies in Section 6.

5.1. SPH discretization

In SPH, the discrete equations are constructed by enforcing the kernel approximation to the governing equations at each node (or particle) in the domain. Randles and Libersky[4] use the following discrete form of the momentum equation (81) with $\mathbf{b}(x)=0$

$$\frac{\mathrm{d}\mathbf{v}_J}{\mathrm{d}t}=\left(-\sum_I \boldsymbol{\nabla}W_{JI}\otimes(\boldsymbol{\sigma}_I-\boldsymbol{\sigma}_J)\frac{m_I}{\rho_J\rho_I}\right):\mathbf{B} \tag{85}$$

where **B** is the derivative correction matrix (69). This form is similar to a discretization by collocation at the points x_J with (68) used as the discrete divergence of stress.

In standard SPH, the gradient of the velocity field is given by (30)

$$\boldsymbol{\nabla}\mathbf{v}(\mathbf{x}_J)=-\sum_I \boldsymbol{\nabla}W_{JI}\mathbf{v}_I\Delta V_I \tag{86}$$

while a 'symmetrized' form with normalization is

$$\boldsymbol{\nabla}\mathbf{v}(\mathbf{x}_J)=\left(-\sum_I \boldsymbol{\nabla}W_{JI}(\mathbf{v}_I-\mathbf{v}_J)\Delta V_I\right):\mathbf{B} \tag{87}$$

When the smoothing length s is identical for all nodes, (87) is equivalent to

$$\boldsymbol{\nabla}\mathbf{v}(\mathbf{x}_J)=\left(\sum_I \boldsymbol{\nabla}W_{IJ}(\mathbf{v}_I-\mathbf{v}_J)\Delta V_I\right):\mathbf{B} \tag{88}$$

where the identity (31) has been used.

5.2. Galerkin methods

We next consider discretization by a Petrov–Galerkin method. The discrete equations are obtained from the weak form of the momentum equation, which is given by

$$\int_\Omega \boldsymbol{\nabla}\boldsymbol{\delta}\mathbf{v} : \boldsymbol{\sigma}\,\mathrm{d}\Omega - \int_\Omega \boldsymbol{\delta}\mathbf{v}\cdot(\mathbf{b}-\rho\dot{\mathbf{v}})\,\mathrm{d}\Omega - \int_{\Gamma_t}\boldsymbol{\delta}\mathbf{v}\cdot\bar{\boldsymbol{\tau}}\,\mathrm{d}\Gamma = 0 \tag{89}$$

where $\boldsymbol{\delta}\mathbf{v}\in\mathscr{V}_0$ are the test functions and $\mathbf{v}\in\mathscr{V}_1$ are the trial functions; the test-and-trial functions in a Petrov–Galerkin method are not the same. The spaces $\mathscr{V}_1$ and $\mathscr{V}_0$ are given by

$$\mathscr{V}_1 = \{\mathbf{v}|\mathbf{v}\in H^1(\Omega), \mathbf{v}=\bar{\mathbf{v}} \quad \text{on } \Gamma_v\} \tag{90}$$

$$\mathscr{V}_0 = \mathscr{V}_1 \cap \{\boldsymbol{\delta}\mathbf{v}|\boldsymbol{\delta}\mathbf{v}=0 \quad \text{on } \Gamma_v\} \tag{91}$$

The test functions and trial functions are approximated as follows:

$$\boldsymbol{\delta}\mathbf{v}^h(\mathbf{x}) = \sum_J \Psi_J(\mathbf{x})\boldsymbol{\delta}\mathbf{v}_J \tag{92}$$

$$\mathbf{v}^h(\mathbf{x},t) = \sum_J \Phi_J(\mathbf{x})\mathbf{v}_J(t) \tag{93}$$

The discrete equations are obtained by substituting (92) and (93) into (89)

$$-\int_\Omega \boldsymbol{\nabla}\Psi_J\cdot\boldsymbol{\sigma}\,\mathrm{d}\Omega + \int_{\Gamma_t}\Psi_J\bar{\boldsymbol{\tau}}\,\mathrm{d}\Gamma + \int_\Omega \Psi_J\mathbf{b}\,\mathrm{d}\Omega = \sum_I \int_\Omega \rho\Psi_J(\mathbf{x})\Phi_I(\mathbf{x})\,\mathrm{d}\Omega\frac{\mathrm{d}\mathbf{v}_I}{\mathrm{d}t} \tag{94}$$

If we now consider the above integrated with nodal quadrature, and the use of a lumped mass approximation, we obtain

$$\sum_{I\in S_J}\{-\boldsymbol{\nabla}\Psi_J(\mathbf{x}_I)\cdot\boldsymbol{\sigma}(\mathbf{x}_I)\Delta V_I + \Psi_J(\mathbf{x}_I)\bar{\boldsymbol{\tau}}(\mathbf{x}_I)\Delta\Gamma_I + \Psi_J(\mathbf{x}_I)\mathbf{b}(\mathbf{x}_I)\Delta V_I\} = m_J\frac{\mathrm{d}\mathbf{v}_J}{\mathrm{d}t} \tag{95}$$

where the set S_J is all nodes whose support include node J, and $m_J=\rho_J\Delta V_J$. In the above, the nodal quadrature weights have been set to the nodal volumes ΔV_I, with $\Delta\Gamma_I$ for boundary integrals. The nodal volumes are usually determined by approximate techniques such that $\sum_I \Delta V_I = V$.

We will consider two methods:

1. A corrected derivative method, based on Krongauz and Belytschko,[8] which is discretized by the Petrov–Galerkin procedure with integrable test functions
2. A Bubnov–Galerkin method using a moving least-squares approximation, where the test functions are integrable and complete up to at least zeroth-order and the trial functions are first order complete.

5.2.1. Corrected derivative method

We let the test functions be the Shepard functions, i.e. $\Psi_I(\mathbf{x}) = w_I^{\mathrm{S}}(\mathbf{x})$ given by (39) and the trial functions be the corrected derivative functions, so that

$$\boldsymbol{\delta}v^h = \sum_I w_I^{\mathrm{S}}(\mathbf{x})\delta\mathbf{v}_I \tag{96}$$

$$\mathbf{v}^h_{,i} = \sum_I G_{iI}(\mathbf{x})\mathbf{v}_I(t) \tag{97}$$

Table I. Discrete momentum equation and velocity gradient expressions for various particle methods

Method	Momentum equation	Velocity gradient
SPH	$\mathbf{v}_J \mathrm{d}t = -\sum_I \nabla W_{JI} \cdot \boldsymbol{\sigma}_I \Delta V_I$	$\nabla v_J = -\sum_I \nabla W_{JI} \mathbf{v}_I \Delta V_I$
SPH (symmetrized)	$\frac{\mathrm{d}\mathbf{v}_J}{\mathrm{d}t} = -\sum_I \nabla W_{JI} \cdot (\boldsymbol{\sigma}_I - \boldsymbol{\sigma}_J) \Delta V_I$	$\nabla v_J = -\sum_I \nabla W_{JI} (\mathbf{v}_I - \mathbf{v}_J) \Delta V_I$
Randles and Libersky	$\frac{\mathrm{d}\mathbf{v}_J}{\mathrm{d}t} = \left(-\sum_I \nabla W_{JI} \otimes (\boldsymbol{\sigma}_I - \boldsymbol{\sigma}_J) \frac{m_J}{\rho_J \rho_I} \right) : \mathbf{B}$	$\nabla \mathbf{v}(\mathbf{x}_J) = \left(-\sum_I \nabla W_{JI} (\mathbf{v}_I - \mathbf{v}_J) \Delta V_I \right) : \mathbf{B}$
Krongauz and Belytschko	$m_J \frac{\mathrm{d}\mathbf{v}_J}{\mathrm{d}t} = -\sum_I \nabla w_I^{\mathrm{S}}(\mathbf{x}_J) \cdot \boldsymbol{\sigma}_I \Delta V_J$	$\nabla \mathbf{v}(\mathbf{x}_J) = \sum_I \mathbf{G}_I(\mathbf{x}_J) \mathbf{v}_I$

Then at an interior node outside of the domain of influence of surface tractions, with no body force, we obtain

$$m_J \frac{\mathrm{d}\mathbf{v}_J}{\mathrm{d}t} = -\sum_{J \in S_I} \nabla w_J^{\mathrm{S}}(\mathbf{x}_I) \cdot \boldsymbol{\sigma}_I \Delta V_I \tag{98}$$

The stress rate for the case of elasticity is given then by (82) with

$$\nabla \mathbf{v}(\mathbf{x}_J) = \sum_I \mathbf{G}_I(\mathbf{x}_J) \mathbf{v}_I \tag{99}$$

Comparing (85) with (98) and (88) with (99) we see that the two discretizations are similar except that $\nabla W_J(\mathbf{x}_I)(\boldsymbol{\sigma}_I - \boldsymbol{\sigma}_J)$ in the Randles and Libersky formulation has been replaced by $\nabla w_J^{\mathrm{S}}(\mathbf{x}_I)\boldsymbol{\sigma}_I$. In Krongauz and Belytschko[8] poor convergence results are reported for the case when corrected derivatives were used as both the test and trial functions. This was attributed to the fact that corrected derivatives are not integrable.

The discrete forms of the momentum equation and the velocity gradient for the various methods presented in this section are shown in Table I.

5.2.2. MLS method

A second way to construct the discrete equations is to use an MLS approximation as in the Element-free Galerkin method (EFG), see Reference 14. Since the MLS functions are integrable, a standard Galerkin method can be used. The discrete equations are then given by (95) with identical test and trial functions given by (44).

5.2.3. Comparison—operations count

The only advantage of corrected derivative approximations over MLS approximations appears to be a reduction in the number of computations. We give here computation estimates for the MLS method and corrected derivative methods for the computation of the function and its derivatives at a node.

We make no distinctions between additions and multiplications. The results are reported in Table II. In Section 6 we give some timings.

Table II. Operation counts for different corrected approximation methods with n denoting the number of neighbours, C_w — cost of evaluation of weight function and its derivatives

Method	Op. count
Corrected approximation, MLS	$nC_w + 101n + 32$
Corrected derivative, Section 4.4.3	$nC_w + 28n + 10$
Corrected derivative, Methods 2 and 3	$nC_w + 41n + 32$

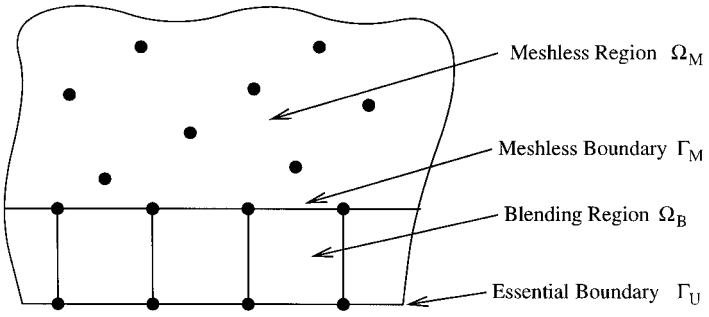

Figure 1. Row of finite elements along an essential boundary in 2D

5.2.4. Enforcement of essential boundary conditions

In Galerkin methods, the test functions must vanish on the prescribed displacement boundaries. The following procedure, a modification of Krongauz and Belytschko,[16] is used to prescribe fixed displacement conditions. A layer of linear finite elements is introduced along the displacement boundary as in Figure 1. A blending function is used between the finite elements on the boundary and the meshfree nodes in the interior. The shape functions in the blending region are given by

$$\Phi_I^0(\mathbf{x}) = \begin{cases} (1 - r(\mathbf{x}))N_I(\mathbf{x}) + r(\mathbf{x})\Phi_I(\mathbf{x}), & \mathbf{x}_I \in \Omega_B \\ r(\mathbf{x})\Phi_I(\mathbf{x}), & \mathbf{x}_I \notin \Omega_B \end{cases} \tag{100}$$

with derivatives

$$\Phi_{I,i}^0 = \begin{cases} -r_{,i}N_I + (1 - r)N_{I,i} + r_{,i}\Phi_I + r\Phi_{I,i}, & \mathbf{x}_I \in \Omega_B \\ r_{,i}\Phi_I + r\Phi_{I,i}, & \mathbf{x}_I \notin \Omega_B \end{cases} \tag{101}$$

where $N_I(\mathbf{x})$ is the finite element shape function associated with node I; $r(\mathbf{x})$ is a blending function which vanishes on the displacement boundary and is unity in Ω_M. It is constructed with the use of a linear ramp function defined as

$$R(\mathbf{x}) = \sum_J N_J(\mathbf{x}) \tag{102}$$

where the summation is over all nodes on the interface Γ_M. This gives $R(\mathbf{x}) = 1$ on Γ_M and $R(\mathbf{x}) = 0$ on Γ_u. The smooth blending function and its derivatives[20] are given by

$$r(\mathbf{x}) = 3R^2(\mathbf{x}) - 2R^3(\mathbf{x}) \tag{103}$$

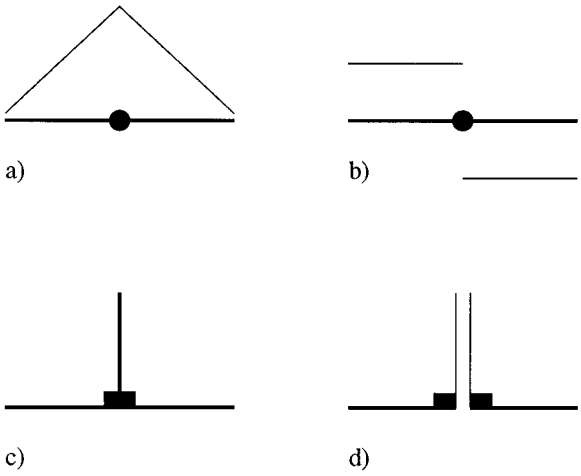

Figure 2. Implementation of nodal integration at boundary nodes. (a) Approximation at a boundary node and (b) its derivative. The volume associated with the node (c) is split into two (d) and contributions from approximation derivatives at both sides of the discontinuity are made to the discrete equations

$$r_{,i}(\mathbf{x}) = (6R(\mathbf{x}) - 6R^2(\mathbf{x}))R_{,i} \tag{104}$$

With nodal integration, the above blending function does not need to be constructed to assemble the discrete equations. Since variables are evaluated only at the nodes, the blending shape functions (100) and their derivatives (101) will only be evaluated at the boundaries of the blending region Ω_B. In this case, with the use of the smooth ramp function, the approximation reduces to

$$\Phi_I^0(\mathbf{x}) = \begin{cases} N_I(\mathbf{x}), & \mathbf{x}_I \in \Omega_B \\ 0, & \mathbf{x}_I \notin \Omega_B \end{cases} \quad \text{on } \Gamma_u \tag{105a}$$

$$\Phi_I^0(\mathbf{x}) = \Phi_I(\mathbf{x}) \quad \text{on } \Gamma_M \tag{105b}$$

since $r = 1$ on Γ_M and $r = 0$ on Γ_u

One difficulty with the above formulation is that the derivatives of the finite element shape functions, $N_{I,i}$ are discontinuous at nodes. Therefore, in integrating the discrete equations, the contributions from finite element nodes are treated as follows. Consider a finite element shape function and its derivatives at a boundary node as shown in Figure 2. We split the weight (or volume) associated with the node amongst the boundary finite elements which contain that node. In forming the discrete equations, the integrals are evaluated in each of the elements. The element integrals are then assembled to the nodes.

5.3. Conservation laws and completeness

5.3.1. Conservation of linear momentum

We show that in the absence of external forces *constant reproducing conditions imply that linear momentum is conserved* while *linear reproducing conditions imply that angular momentum is conserved*. Conservation of linear momentum requires that the rate of change of linear momentum equal the total force applied to the body or system of particles, or that the total change of linear

momentum due to internal forces is zero. Thus in the absence of external forces conservation of linear momentum requires that

$$\frac{\mathrm{d}}{\mathrm{d}t}\left(\sum_I m_I \mathbf{v}_{Ii}\right) = \sum_I m_I \dot{\mathbf{v}}_{Ii} = 0 \tag{106}$$

where the m_I are nodal masses. In the absence of tractions and body forces the acceleration is given by (94), which is rewritten as

$$m_I \dot{v}_{Ii} = -\sum_J \Psi_{I,j}(\mathbf{x}_J)\sigma_{ji}(\mathbf{x}_J)\Delta V_J \tag{107}$$

To determine the conditions the shape functions must satisfy in order for the Galerkin semi-discrete equations to conserve linear momentum, we substitute the discrete Galerkin equations (107) into (106)

$$\sum_I m_I \dot{v}_{Ii} = -\sum_I \sum_J \Psi_{I,j}(\mathbf{x}_J)\sigma_{ji}(\mathbf{x}_J)\Delta V_J = -\sum_J \underbrace{\sum_I \Psi_{I,j}(\mathbf{x}_J)}_{=0}\sigma_{ji}(\mathbf{x}_J)\Delta V_J = 0 \tag{108}$$

where the constant reproducing conditions (6a) of the shape function derivatives were used. Thus, we have shown that constant reproducing conditions result in a discretization that conserves linear momentum.

5.3.2. *Conservation of angular momentum*

Conservation of angular momentum requires that any change in angular momentum is due exclusively to external forces. We will show that the change in angular momentum in the absence of external forces vanishes. The time rate of change of angular momentum can be expressed as

$$\frac{\mathrm{d}}{\mathrm{d}t}\left(\sum_I m_I \mathbf{v}_I \times \mathbf{x}_I\right) = \sum_I m_I(\dot{\mathbf{v}}_I \times \mathbf{x}_I + \underbrace{\mathbf{v}_I \times \mathbf{v}_I}_{=0}) = 0 \tag{109}$$

in the absence of external forces. Here $\times$ denotes the vector cross product. Substituting (107) into (109) we obtain

$$\frac{\mathrm{d}}{\mathrm{d}t}\left(\sum_I m_I \mathbf{v}_I \times \mathbf{x}_I\right) \cdot \mathbf{e}_i = \sum_I \varepsilon_{ijk}\left(\sum_J \Psi_{I,m}(\mathbf{x}_J)\sigma_{mj}(\mathbf{x}_J)\Delta V_J\right) x_{Ik} \tag{110}$$

where ε_{ijk} is the permutation symbol and x_{Ik} refers to the kth component of particle I; a sum over repeated indices is implied. The sum can be taken inside the integral in (110) to yield

$$\varepsilon_{ijk}\sum_J \underbrace{\left(\sum_I \Psi_{I,m}(\mathbf{x}_J)x_{Ik}\right)}_{=\delta_{mk}}\sigma_{mj}(\mathbf{x}_J)\Delta V_J = \varepsilon_{ijk}\delta_{mj}\sum_J \sigma_{mj}(\mathbf{J})\Delta V_J = \sum_J \underbrace{\varepsilon_{ijm}\sigma_{mj}(\mathbf{x}_J)}_{=0}\Delta V_J = 0 \tag{111}$$

where the linear reproducing conditions (7) of the derivatives of the approximation and the symmetry of the Cauchy stress tensor were used. Thus angular momentum is conserved if the shape functions possess linear completeness.

6. NUMERICAL EXAMPLES

SPH is generally used in Lagrangian hydrocodes and very few problems which can be solved by these programs have closed-form solutions. This has hampered the examination of the accuracy and convergence characteristics of the methods. The following studies are motivated by the argument that if a method is convergent, it must be convergent for the simplest subset of problems which are encompassed in the problem domains. For particle methods applicable to non-linear mechanics, a simple subset is linear elasticity. A method for the continuum mechanics of a transient response cannot be convergent if it fails to converge for static, linear elasticity problems. Therefore, the convergence of a discretization method in static, linear elastic problems is necessary if the discretization is to converge for non-linear problems. In linear elasticity, a number of closed-form solutions are available, so the convergence of a discretization can be studied numerically. Although convergence in a small set of problems does not insure convergence in general, the absence of convergence clearly indicates that a method is flawed. Thus showing lack of convergence of specific methods numerically suffices to demonstrate a defect in the discretization.

6.1. A note on the convergence properties of SPH

Convergence has been proven for SPH and similar particle methods for linear hyperbolic and parabolic systems by Mas-Gallic and Raviart.[21] In the following, we argue that this proof does not apply to particle methods as they are generally used.

There are two sources of error associated with the discrete form of the kernel approximation to a function (21), the error associated with the smoothing procedure and the error associated with the approximate integration of (21). If the kernel is an even function, the smoothing procedure is second-order accurate in s

$$\langle u(x)\rangle = u(x) + O(s^2) \tag{112}$$

The integration error associated in going from the continuous form of the kernel (19) to the discrete form (21) depends on the nodal arrangement. The minimum error results when the nodes are spaced uniformly. The truncation error ε in this case for the nth-order derivative of a function is given by

$$\varepsilon = O\left(s^{-n}\left(\frac{\Delta x}{s}\right)^2\right) \tag{113}$$

(Reference 22). Combining the smoothing error (112) with the integration error (113) shows that a method converges with a rate of $s^2 + s^{-n}(\Delta x/s)^2$. This is the same estimate given in Mas-Gallic and Raviart.[21]

This estimate implies that convergence in standard SPH requires that $s^{-n}(\Delta x/s)^2 \to 0$ as both Δx and $s \to 0$. For a first-order (or higher-order) PDE this requires $s \to 0$ much more slowly than Δx. As a consequence, the number of neighbors N grows rapidly as the discretization is refined since $N \propto (s/\Delta x)$. We have verified convergence under these conditions in one-dimensional numerical studies. However, these conditions require the number of nodes in the support of the kernel to increase markedly with refinement, so that the sparsity of the equations deteriorates. Moreover, the cost of constructing the approximation at each point dramatically increases. If the completeness corrections described here are made to the kernel, the discretization converges even if s is decreased in direct proportion with Δx as the examples in this section will show. In the

following convergence studies, the ratio $(\Delta x/s)$ is kept constant as the discretizations are refined, so the same sparsity is maintained.

6.2. Static problems

In this section several problems are solved by the techniques described in this paper. Solutions are reported for the following approximating functions:

1. the symmetrization correction (47) on both the gradient of the displacement and divergence of the stress fields, as commonly used in SPH (SPH);
2. the Johnson–Beissel correction for the gradient of the stress and displacement fields used for the test and trial functions (JB);
3. the Randles–Libersky correction (RL);
4. the method proposed here in which the trial function derivatives are the corrected derivatives (55) (CD1);
5. corrected derivative method (Method 2) (63) where linear completeness is imposed on the trial function (CD2);
6. moving least-squares approximation with linear completeness on both the approximating function and its derivative (MLS); and
7. element free Galerkin method, where a background cell and 5×5 Gaussian quadrature has been used to evaluate the Galerkin integrals[14] (EFG).

For cases 1–3, 6 and 7, a Bubnov–Galerkin method was used with the test and trial functions identical and as listed. For cases 4 and 5, a Petrov–Galerkin method was used with a Shepard test function and the functions listed as trial functions. Nodal quadrature was used to evaluate the weak form in cases 1–6.

Two error norms were used in the convergence studies. An approximate l_2 error in displacement is computed by

$$\text{error}_{l_2} = \frac{l_2(u^h - u^{\text{exact}})}{l_2(u^{\text{exact}})} \tag{114}$$

where

$$l_2(u) = \left(\sum_{I=1}^{n} u_I^2 \Delta V_I \right)^{1/2} \tag{115}$$

The above is an error measure which applies only to nodal values. This norm may converge even if the displacement fields associated with the discrete solutions do not converge.

We also check convergence in the L_2 and energy norms:

$$\text{error}_{L_2} = \frac{\|u^h - u^{\text{exact}}\|_{L_2}}{\|u^{\text{exact}}\|_{L_2}} \tag{116}$$

$$\|u\|_{L_2} = \left(\int_\Omega u_i u_i \, \mathrm{d}\Omega \right)^{1/2} \tag{117}$$

$$\text{error}_{rmEnergy} = \frac{\|u^h - u^{exact}\|_{\text{Energy}}}{\|u^{\text{exact}}\|_{\text{Energy}}} \tag{118}$$

$$\|u\|_{\text{Energy}} = \left(\int_\Omega \boldsymbol{\nabla}\mathbf{u} : \mathbf{C} : \boldsymbol{\nabla}\mathbf{u} \, \mathrm{d}\Omega \right) \tag{119}$$

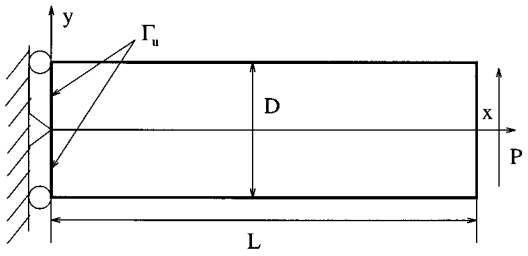

Figure 3. Cantilever beam

where **C** is the fourth-order elasticity tensor. The integrals were evaluated by Gaussian 5×5 quadrature.

6.2.1. Cantilever beam

The solution for a cantilever beam subject to an end load as shown in Figure 3 is given by Gere and Timoshenko[23] as

$$u_x = \frac{-Py}{6EI}\left[(6L - 3x)x + (2 + \nu)\left(y^2 - \frac{D^2}{4}\right)\right] \tag{120}$$

$$u_y = \frac{P}{6EI}\left[3\nu y^2(L - x) + (4 + 5\nu)\frac{D^2 x}{4} + (3L - x)x^2\right] \tag{121}$$

The stresses are given by

$$\sigma_{xx} = -\frac{P(L - x)y}{I} \tag{122}$$

$$\sigma_{yy} = 0 \tag{123}$$

$$\sigma_{xy} = \frac{P}{2I}\left(\frac{D^2}{4} - y^2\right) \tag{124}$$

where I is the moment of inertia. For a beam with rectangular cross-section and unit thickness I is given by

$$I = \frac{D^3}{12} \tag{125}$$

where D is the width of the beam. The displacements (120) and (121) are prescribed as essential boundary conditions at $x = 0$, $-D/2 \leqslant y \leqslant D/2$; the remaining boundaries are traction boundaries. A typical nodal arrangement used in the convergence study is shown in Figure 4; note the single row of the finite elements adjacent to the essential boundary on the left which are used to enforce the essential boundary conditions.

The following parameters were used for the cantilever beam problem: $E = 1000$; $\nu = 0{\cdot}3$; $D = 1$; $L = 8$. Regular nodal arrangements with uniform nodal spacing were used. The smoothing length s was chosen to be the diagonal distance between nodes

$$s = \sqrt{2}\Delta x = \sqrt{2}\Delta y \tag{126}$$

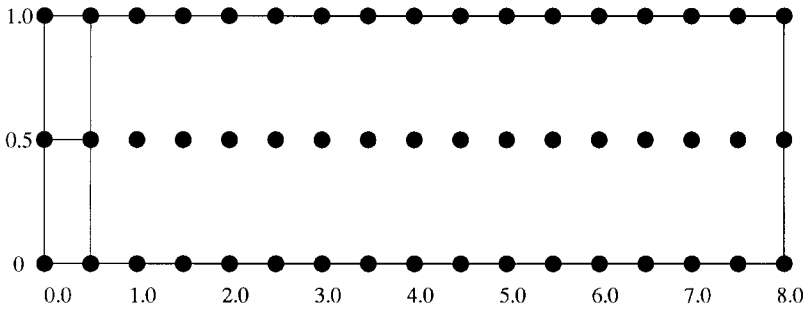

Figure 4. A sample nodal arrangement and elements used for the beam problem

Table III. Convergence rates for the cantilever beam and plate with hole problems. 'NC' implies that no convergence was observed

Problem	Beam		Plate with hole	
Method	Energy	L_2	Energy	L_2
SPH	NC	NC	NC	NC
Johnson and Beissel correction (JB)	NC	NC	NC	NC
Randles and Libersky correction (RL)	0·98	0·41	0·51	0·62
Corrected Derivatives I (CD1)	1·29	1·84	0·54	1·10
Corrected Derivatives II (CD2)	1·29	1·84	0·49	1·30
Moving-Least Squares (MLS)	1·50	1·82	0·65	1·22
EFG (MLS with background quadrature)	1·50	2·00	1·50	2·50

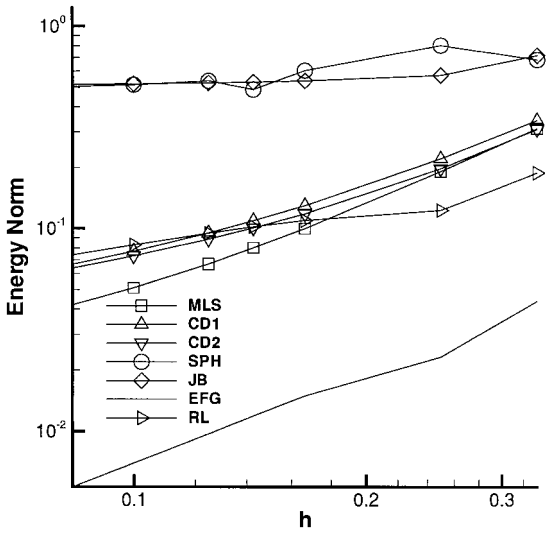

Figure 5. Convergence in strain energy for the cantilever beam problem: SPH—symmetrized smooth particle hydrodynamics, JB—SPH with Johnson–Beissel correction, CD1—first derivative correction, CD2 second derivative correction, MLS—full linear reproducing correction on both functions and derivatives, EFG—Element Free Galerkin

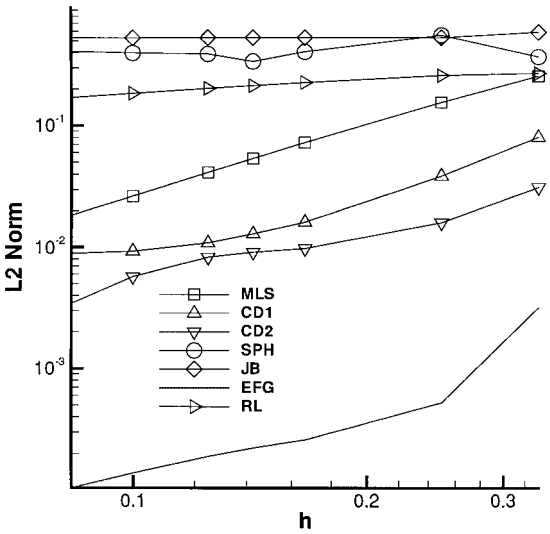

Figure 6. Convergence of L_2 norm in displacements for the cantilever beam problem: SPH—symmetrized smooth particle hydrodynamics, JB—SPH with Johnson–Beissel correction, CD1—first derivative correction method, CD2—second derivative correction, MLS—full linear reproducing correction on both functions and derivatives, EFG—Element Free Galerkin

and the kernel function was chosen to be the B-spline (26). This smoothing length results in an average of 21 neighbours for nodes on the interior of the model.

The seven methods described in the beginning of Section 6 were used to correct the completeness of the kernel approximations. The convergence rates are summarized in Table III, and the results are shown in Figures 5 and 6.

6.2.2. Plate with a hole

The solution for the infinite plate with a hole subject to a unit traction in the x direction at infinity is given in Timoshenko and Goodier[24] as

$$\sigma_{xx} = 1 - \frac{a^2}{r^2}\left(\tfrac{3}{2}\cos(2\theta) + \cos(4\theta)\right) + \frac{3a^4}{2r^4}\cos(4\theta) \tag{127}$$

$$\sigma_{yy} = -\frac{a^2}{r^2}\left(\tfrac{1}{2}\cos(2\theta) - \cos(4\theta)\right) - \frac{3a^4}{2r^4}\cos(4\theta) \tag{128}$$

$$\sigma_{xy} = -\frac{a^2}{r^2}\left(\tfrac{1}{2}\sin(2\theta) + \sin(4\theta)\right) + \frac{3a^4}{2r^4}\sin(4\theta) \tag{129}$$

Only the upper quadrant of the problem is modelled as shown in Figure 7. The tractions from the exact solution are applied to the outer boundaries of the model, and zero normal displacements are prescribed on the symmetry boundaries.

The following parameters were used: $E = 1000$; $v = 0{\cdot}3$; $a = 1$; $b = 5$. The smoothing length s, was computed by

$$s = \sqrt{2}\Delta x^{\text{boundary}} \tag{130}$$

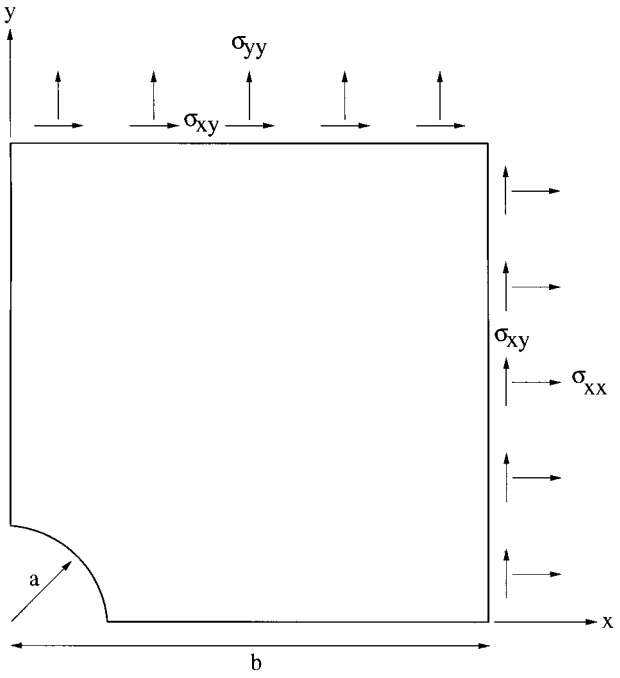

Figure 7. Quarter model used for plate with the hole problem

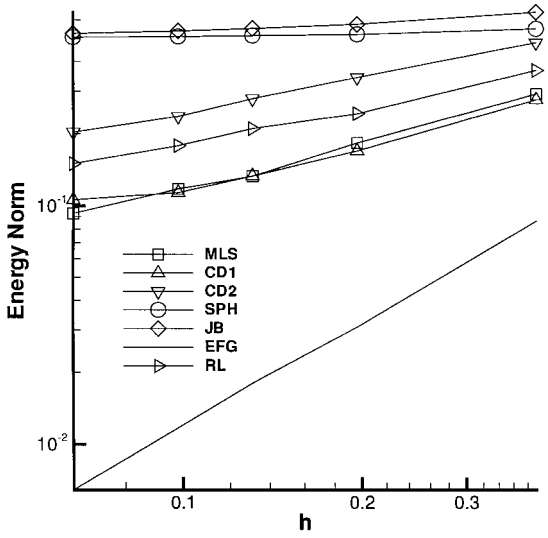

Figure 8. Strain energy convergence plot for the plate with a hole problem

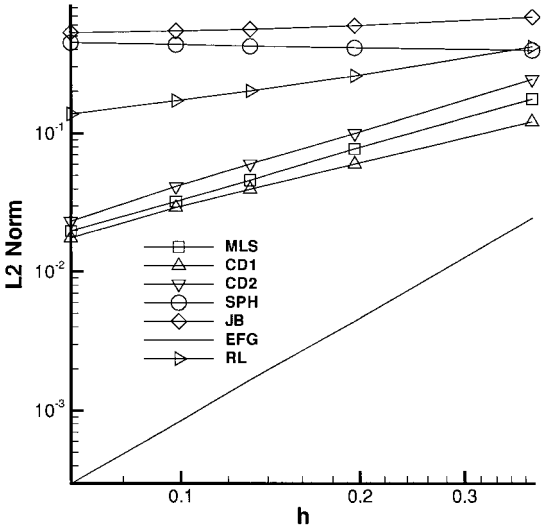

Figure 9. L_2 norm convergence for the plate with a hole problem

where $\Delta x^{\text{boundary}}$ was the nodal spacing along the symmetry boundary. The convergence results are summarized in Table III. The convergence in energy is shown in Figure 8. The convergence in the L_2 norm is shown in Figure 9.

6.2.3. Discussion of results

The results as summarized in Table III show convergence in the l_2 norm for the methods of derivative correction (Reference 8 and the one proposed here) and for the two methods based on moving least-square approximations (MLS and EFG). The Johnson–Beissel[3] correction did improve the SPH accuracy in the energy norm slightly. The accuracy and convergence rates of the two corrected derivative formulations are very close to that of the full MLS correction. The EFG solution is as expected the best overall, but it comes at a greater computational price due to the use of background integration.

The accuracy and rate of convergence for both corrected derivative methods are similar to those observed with the full MLS correction. The results for the Randles–Libersky correction are inconclusive. The error in strain energy for the hole problem is of the same order or better than for MLS or the two corrected derivative methods, but the L_2 norm in both problems was quite inaccurate. The lack of convergence of these methods[3, 4] is attributed to two factors:

1. as mentioned in Section 4.4.6, the Johnson and Beissel correction does not restore the full completeness of the derivatives;
2. test functions using Randles and Libersky[4] correction are not integrable, as discussed in Section 4.4.6.

Although the Randles and Libersky[4] discretization is not developed by a Galerkin methodology, since the discrete equation is almost identical to the Petrov–Galerkin, we expect it to be subject to the same restrictions.

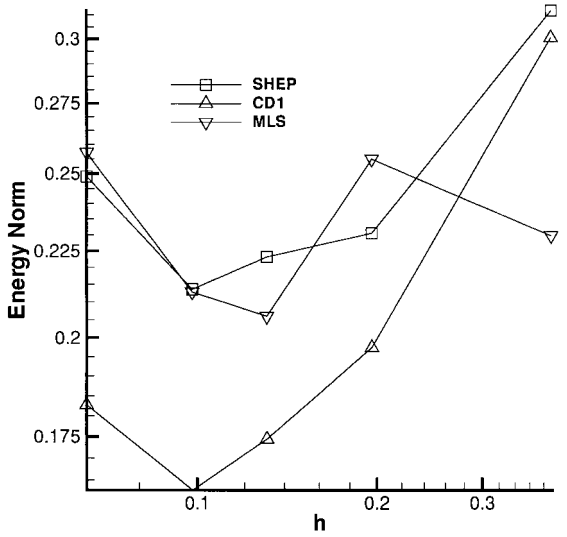

Figure 10. Energy norm convergence for the plate with a hole problem. The discrete equations were constructed using nodal quadrature, while the energy norm was evaluated using full integration

The rather low absolute accuracy of all the corrected derivatives methods, as compared for example to EFG with background quadrature, is attributed to the integration error associated with nodal integration, which is characteristic of all particle methods. The convergence rates observed in the hole problem were much lower than in the beam problem. This may be due to the non-uniform arrangements of the nodes in the latter. The EFG method with background cell quadrature shows a much greater convergence rate and better absolute accuracy as expected.

It is noteworthy that whereas the error in energy as measured by an l_2 norm over the nodal values converged, the L_2 norm of the error is more erratic, as shown in Figure 10. Here MLS Galerkin, which is first-order complete, does not converge, whereas Shepard Galerkin and Petrov–Galerkin with corrected derivatives (Method 1) also do not converge. This behavior is attributable to deficiencies in the stability of the discretization obtained by nodal quadrature. The results for strains exhibited oscillations between nodes, which are evidence of a lack of stability. It is remarkable that the l_2 norms (i.e. the error on the nodes) is as well behaved as they are.

To estimate the effects of instabilities, we also show the L_2 errors in strain for discretizations obtained with background quadrature (5×5 gauss quadrature on quadrilaterals generated by the nodes). These results, Figure 11, show excellent convergence for the corrected derivative and MLS approximations. These results are more indicative of the ultimate capability of the tested approximations, but they are not as pertinent to true particle methods, where quadrature needs to be restricted to nodes.

6.3. Dynamic problems

An end loaded cantilever beam was chosen as the test problem for the dynamic case. The setup is illustrated in Figure 3 with

$$P = 15(1 - 1/4y^2) \tag{131}$$

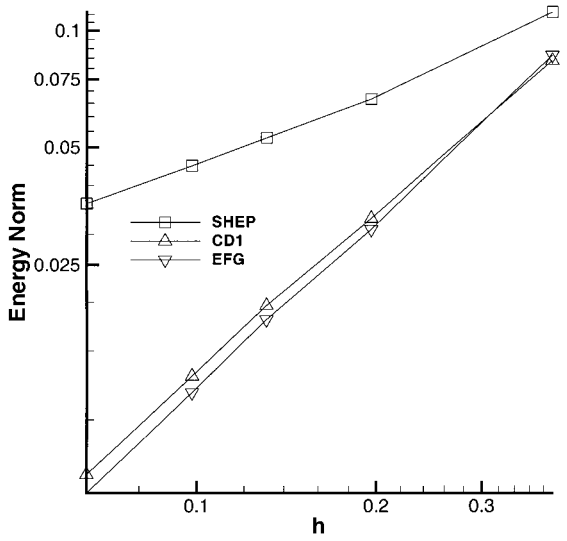

Figure 11. Energy norm convergence for the plate with a hole problem. Both the construction of the discrete equations and the calculation of the energy norm used full background integration

$$D = 4 \tag{132}$$

$$L = 25 \tag{133}$$

The problem parameters used were: $v = 0{\cdot}25$, $E = 10^4$, E_p (plastic hardening modulus) $= 100$ and σ_y (yield stress) $= 300$, This problem was studied in Belytschko and Bindeman.[25] The following approximations were used for this problem:

1. Element-Free Galerkin method (EFG);
2. Petrov–Galerkin with Shepard functions as test functions and the corrected derivatives given in Section 4.4.3 as trial function derivatives (CD1);
3. same as 2, but with corrected derivatives of the form of Section 4.4.5 (CD2).

Three initially regular meshes were used for this problem with dimensions 25×4, 33×7, and 55×10. The results for the case of 2×2 Gaussian cell quadrature are given in Figure 12. It can be seen in the figure that both corrected derivative methods converge to the EFG solution as the mesh is refined, the EFG is considered a benchmark solution. There is little difference in accuracy between the two corrected derivative formulations, which is similar to what was observed for static problems. Galerkin EFG with nodal quadrature was used to solve this problem on the three meshes (25×4, 33×7, 55×10) and compared with the solution obtained by 2×2 Gaussian cell quadrature. In the absence of artificial viscosity the solution for all cases of nodal quadrature exhibited marked instabilities. The conservative smoothing technique of Randles and Libersky[4] with a smoothing coefficient of 0·1 was sufficient to prevent instabilities. The results are plotted in Figure 13. It can be seen from the figure that nodal quadrature results improve as the mesh is refined. Particles positions at time $t = 10$ s are shown in Figure 14.

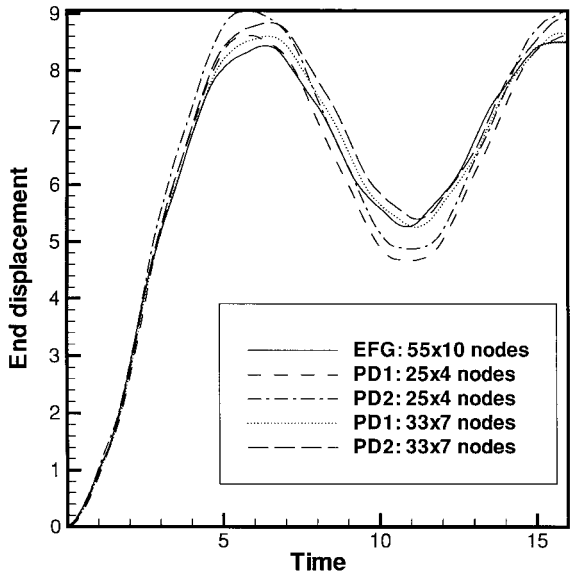

Figure 12. Time history of end displacement for elastoplastic cantilever beam

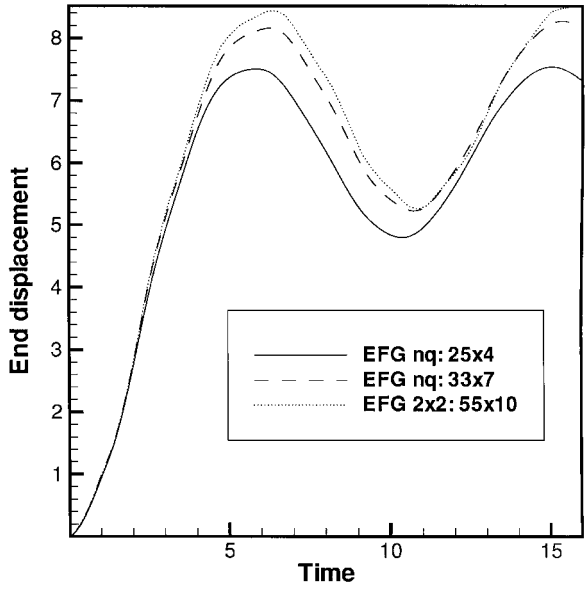

Figure 13. Time history of the end displacement of cantilever beam; comparison of nodal quadrature with conservative smoothing with 2×2 quadrature

6.4. Timings

The timing results for computing the shape functions by two techniques: MLS[14] and the corrected derivatives of Section 4.4.3 are presented in Table IV. When the support of the weight function

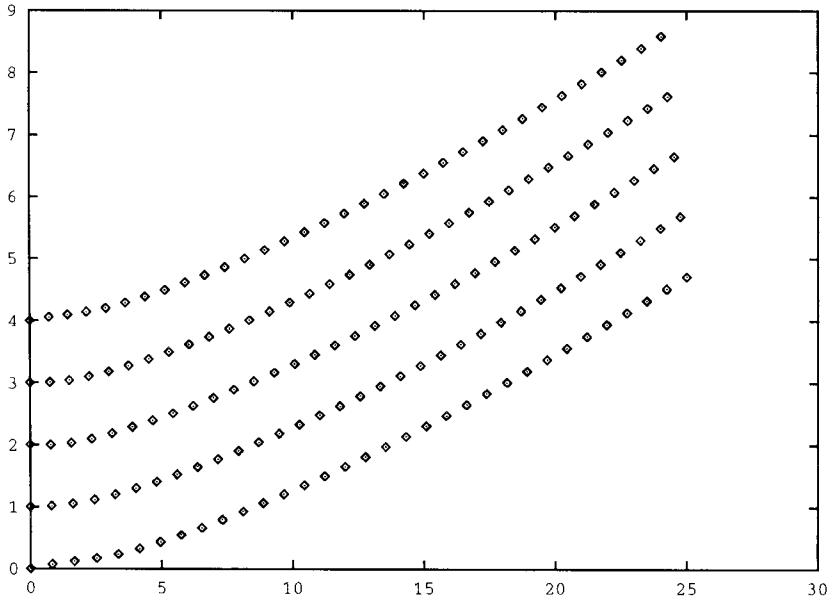

Figure 14. Particle positions at 10 s for the cantilever beam problem

Table IV. Speedup factors of corrected derivative formulation over MLS

Domain size multiplier	Speedup factor
$d_m = 1{\cdot}5$	3·06
$d_m = 2{\cdot}5$	3·12
$d_m = 3{\cdot}5$	2·43

increases (i.e. the number of neighbours grows) the speedup decreases. However, in practical computations d_m is usually in the range 1·7–2·5.

6.5. *Damage*

The standard SPH method does not work well in the modelling of damage and unstable material behaviour, such as occurs in shear bands. The problem arises because the standard support for the kernel function $W(\mathbf{x}-\mathbf{x}_I, s)$ is too large. When s is greater than the nodal spacing, the behaviour at point $\mathbf{x}_I$ is influenced by material response at more remote nodes. While material instability usually results in localization of the deformation, the deformation fails to localize when s is too large.

Here we propose that with the onset of material instability, the smoothing length should be reduced to a distance corresponding to the nodal spacing. This procedure can be triggered by the indication of instability in the rate-independent moduli or by a critical value of the damage parameter. The support size should be reduced by as much as possible without impairing the regularity of the **A** matrix.

The advantages of this strategy can be seen from Plate 1, which shows the onset and evolution of a shear band in a viscoplastic specimen under compression. Material properties and other problem parameters are given in Belytschko *et al.*[7] Only the upper right-hand quadrant is shown; the response is symmetric. A fine mesh calculation is shown in the bottom two figures and shows the emergence of a shear band in the middle of the plate (lower left corner of the symmetric model). This is the benchmark solution which has been confirmed with finer meshes and finite element solutions.

It can be seen that when the support size is relatively large, the shear band is wider than with the smaller support size. Furthermore, later in the simulation, other areas of localization develop. Thus it is clear that to capture the localization of deformation associated with material instability, the smoothing length, i.e. the support of the kernel function, must be reduced.

7. CONCLUSIONS

The correction for completeness of meshfree approximations such as SPH has been examined by numerically checking rates of convergence for elastic problems. It was found that convergence can be achieved for by either using

(a) approximations for test and trial functions which reproduce linear functions (linear completeness),
(b) trial functions with derivatives corrected so that the derivatives of linear functions are correctly reproduced and test functions which reproduce constant functions and have integrable derivatives.

We have emphasized the reproducing conditions on the approximation because consistency is difficult to check or correct for an unstructured grid of nodes. The reproducing conditions imply completeness, which plays roughly the same role in the convergence of Galerkin methods that consistency plays in finite-difference methods.

We found that standard SPH, even with a symmetrization which ensures zeroth-order completeness, does not converge if the size of the support of the kernel (smoothing length) is kept proportional to the distance between nodes. On the other hand, our results (not reported here) in one dimension agreed with the proof by Raviart which shows convergence when a relationship between the nodal spacing and size of the support is maintained. Of course, the latter leads to a severe decrease in the sparsity of the equations, which dramatically decreases computational efficiency. Furthermore, SPH with normalized derivatives (corrected for linear reproducing conditions) does not appear to converge when the support size is proportional to the nodal spacing. We attribute this behaviour to the lack of integrability in the functions which play the role of test functions in Petrov–Galerkin formulations.

We have also shown that the reproducing conditions imply momentum conservation properties. Test functions that satisfy constant reproducing conditions imply the conservation of linear momentum, while test functions with linear completeness imply the conservation of angular momentum.

In order to effectively model localization associated with material instabilities, such as damage or strain-softening, the support size must be decreased. Otherwise, the influence of nodes where material instabilities have not occured limits the localization. This was shown by calculations of shear band formation in viscoplastic solids.

Particle methods such as SPH, in which approximations are constructed only at the nodes, are attractive because they are truly meshfree; a background quadrature scheme is unnecessary to

integrate the discrete equations. This makes the method much more computationally efficient, but at the cost of a loss in accuracy, and perhaps stability. Stability is marginal in nodal integration, because even when the norm associated with the nodal value converged, oscillations were observed between nodes. In dynamic solutions instabilities were observed with nodal integration in the absence of stabilization procedures. Therefore, effective stabilization techniques are crucial.

ACKNOWLEDGEMENTS

The authors are grateful for the support provided by the Office of Naval Research and the U.S. Army Office of Research, to Northwestern University and the support of the DOE Computational Science Graduate Fellowship program for John Dolbow and Charles Gerlach. This work is also sponsored by the Army High Performance Computing Research Center under the agencies of the Department of the Army, Army Research Laboratory Cooperative Agreement DAAH-04-95-2-003. The content does not reflect the position or policy of the government.

REFERENCES

1. R. Gingold and J. Monaghan, 'Smoothed particle hydrodynamics: theory and application to non-spherical stars', *Mon. Not. Roy. Astron. Soc.*, **181,** 375–389 (1977).
2. W. Liu, S. Jun, S. Li, J. Adee and T. Belytschko, 'Reproducing kernel particle methods for structural dynamics', *Int. J. Numer. Meth. Engng.*, **38,** 1655–1680 (1995).
3. G. R. Johnson and S. R. Beissel, 'Normalized smoothing functions for SPH impact calculations', *Int. J. Numer. Meth. Engng.*, **39,** 2725–2741 (1996).
4. P. Randles and L. Libersky, 'Smoothed Particle Hydrodynamics: Some recent improvements and applications', *Comput. Meth. Appl. Mech. Engng.*, **139,** 375–408 (1996).
5. G. Dilts, 'Moving-least-squares-particle hydrodynamics i: Consistency and stability', *Int. J. Numer. Meth. Engng.*, 1997, Submitted for publication.
6. T. Belytschko, Y. Krongauz, D. Organ, M. Fleming and P. Krysl, 'Meshless methods: an overview and recent developments', *Comput. Meth. Appl. Mech. Engng.*, **139,** 3–47 (1996).
7. T. Belytschko, H. Y. Chiang and E. Plaskacz, 'High resolution two-dimensional shear band computations: imperfections and mesh dependency', *Comput. Meth. Appl. Mech. Engng.*, **119,** 1–15.
8. Y. Krongauz and T. Belytschko, 'Consistent pseudo-derivatives in meshless methods', *Comput Meth. Appl. Mech. Engng.*, **146,** 371–386 (1997a).
9. J. J. Monaghan, 'Smoothed particle hydrodynamics', *Annu. Rev. Astron. Astrophys.*, **30,** 543–574 (1992).
10. T. Hughes, *The Finite Element Method*, Prentice-Hall, Englewood Cliffs, N.J., 1987.
11. J. C. Strikwerda, *Finite Difference Schemes and Partial Differential Equations*, Wadsworth & Brooks, Pacific Grove, CA, 1989.
12. W. G. Strang and G. J. Fix, *An Analysis of Finite Element Method*, Prentice-Hall, Englewood Cliffs, N.J., 1973.
13. D. Shepard, 'A two dimensional function for irregularly spaced data', *ACM National Conf.*, 1968.
14. T. Belytschko, Y. Y. Lu and L. Gu, Element-free Galerkin methods, *Int. J. Numer. Meth. Engng.*, **37,** 229–256.
15. J. Monaghan, 'An introduction to sph', *Comput. Phys. Commun.*, **48,** 89–96 (1988).
16. Y. Krongauz and T. Belytschko, 'Enforcement of essential boundary conditions in meshless approximations using finite elements', *Comput. Meth. Appl. Mech. Engng.*, **131,** 133–145 (1996).
17. J. Morris, 'A study of the stability properties of smooth particle hydrodynamics', *Publ. Astron. Soc. Aust.*, **13** (1996).
18. Y. Krongauz and T. Belytschko, 'An improved diffuse-element meshless method based on a Petrov–Galerkin formulation', *Comput. Mech.*, **19,** 371–333 (1997b).
19. B. Nayroles, G. Touzot and P. Villon, 'Generalizing the finite element method: diffuse approximation and diffuse elements', *Comput. Mech.*, **10,** 307–318 (1992).
20. T. Black, private communication, 1995.
21. S. Mas-Gallic and P. Raviart, 'A particle method for first-order symmetric systems', *Numer. Math.*, **51,** 323–352 (1987).
22. P. Laguna, 'Smoothed particle interpolation', *Astrophys. J.*, **439,** 814–821 (1995).
23. J. M. Gere and S. Timoshenko, *Mechanics of Materials*, 3rd edn, PWS-KENT Pub. Co., Boston, 1990.
24. S. P. Timoshenko and J. N. Goodier, *Theory of Elasticity*, 3rd edn, McGraw-Hill, New York, 1987.
25. T. Belytschko and L. Bindeman, 'Assumed strain stabilization of the 4-node quadrilateral with 1-point quadrature for nonlinear problems', *Comput. Meth. Appl. Mech. Engng.*, **88,** 311–340 (1991).

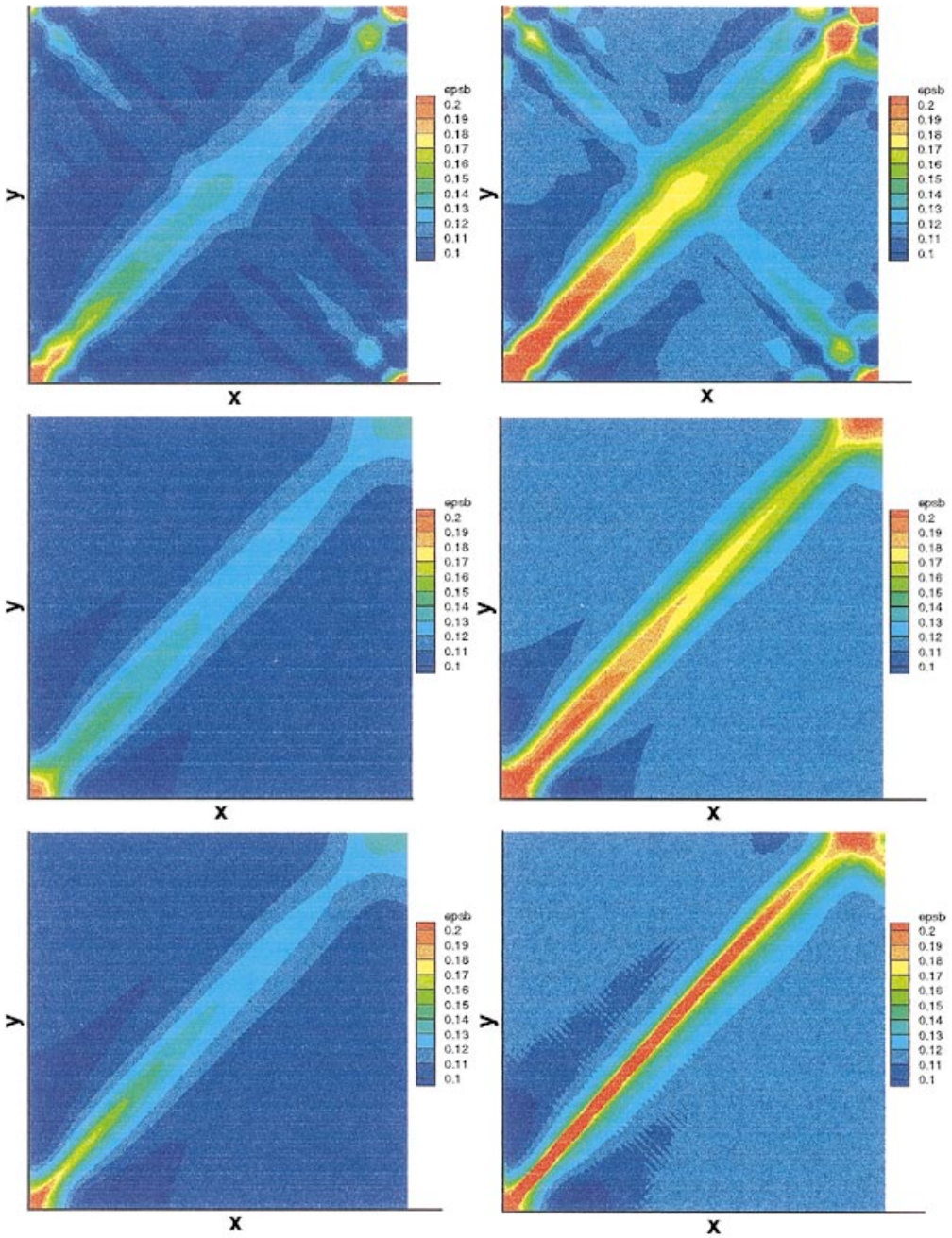

Plate 1. Effective strain contours for a compressed bar with a viscoplastic strain-softening material model; top: $s = 1{\cdot}51h$, 21 x 21 nodes; middle: $s = 0{\cdot}51h$, 21 x 21 nodes; bottom: $s = 0{\cdot}51h$, 81 x 81 nodes; left column at $t = 3{\cdot}24 \times 10^{-6}$, right column at $t = 3{\cdot}76 \times 10^{-6}$